JPL PUBLICATION 79-87

Evaluation of Concentrated Space Solar Arrays Using Computer Modeling

D. E. Rockey

November 1, 1979

National Aeronautics and Space Administration

Jet Propulsion Laboratory
California Institute of Technology
Pasadena, California

JPL PUBLICATION 79-87

Evaluation of Concentrated Space Solar Arrays Using Computer Modeling

D. E. Rockey

November 1, 1979

National Aeronautics and
Space Administration

Jet Propulsion Laboratory
California Institute of Technology
Pasadena, California

The research described in this publication was carried out by the Jet Propulsion Laboratory, California Institute of Technology, under NASA Contract No. NAS7-100.

ABSTRACT

A general approach is developed for predicting the power output of a concentrator enhanced photovoltaic space array. A ray trace routine determines the concentrated intensity arriving at each solar cell. An iterative calculation determines the cell's operating temperature since cell temperature and cell efficiency are functions of one another. The end result of the iterative calculation is that the individual cell's power output is determined as a function of temperature and intensity. Circuit output is predicted by combining the individual cell outputs using the single diode model of a solar cell. Concentrated array characteristics such as uniformity of intensity and operating temperature at various points across the array are examined using computer modeling techniques. An illustrative example is given showing how the output of an array can be enhanced using solar concentration techniques.

CONTENTS

FIGURES

FIGURES

TABLES

INTRODUCTION

The incentive for using a concentrated array is to improve power to mass performance and cost effectiveness. Many different schemes for providing an array with concentrated illumination have been proposed. Systems using lenses, mirrors, or combinations of mirrors and lenses have been suggested. Finding the optimal concentration method for any particular situation (near earth or deep space for example) represents a challenging engineering problem.

The only certain way of determining the performance of a particular concentration method is to actually build a scale model using proposed materials and solar cells. However, the high cost associated with building and testing such scale models makes it more reasonable to first model the power performance of various concentration concepts using computer techniques. Such modeling can dramatically narrow the choice of potential concentration schemes by discarding the least favorable candidates While the modeling approach is general, the modeling results are highly specific, based upon the particular selection of solar cell type, circuit size, circuit orientation and concentrator geometry.

The concentrated array selected for illustration is the compound parabolic concentrator (CPC) in combination with a 2-ohm-cm, 2x2 cm, 50-micron thin silicon solar cell array. The CPC consists of truncated parabolic specular mirrors extending along two sides of the rectangular array. (Reference 1 and 2). The geometric intensity concentration ratio (Cg) can be adjusted by changing the angle of the mirrors to the array (Figure 1). The array selected consists of a single circuit of four cells in parallel by 20 cells in series. Rays entering the concentrator either strike the array directly or are redirected by the mirrors onto the array. The first step in the modeling process is to trace a sufficient number of evenly spaced incident rays to determine the intensity profile across the array. Each successive modeling step, as it applies to this illustrative example, is examined in the subsequent sections.

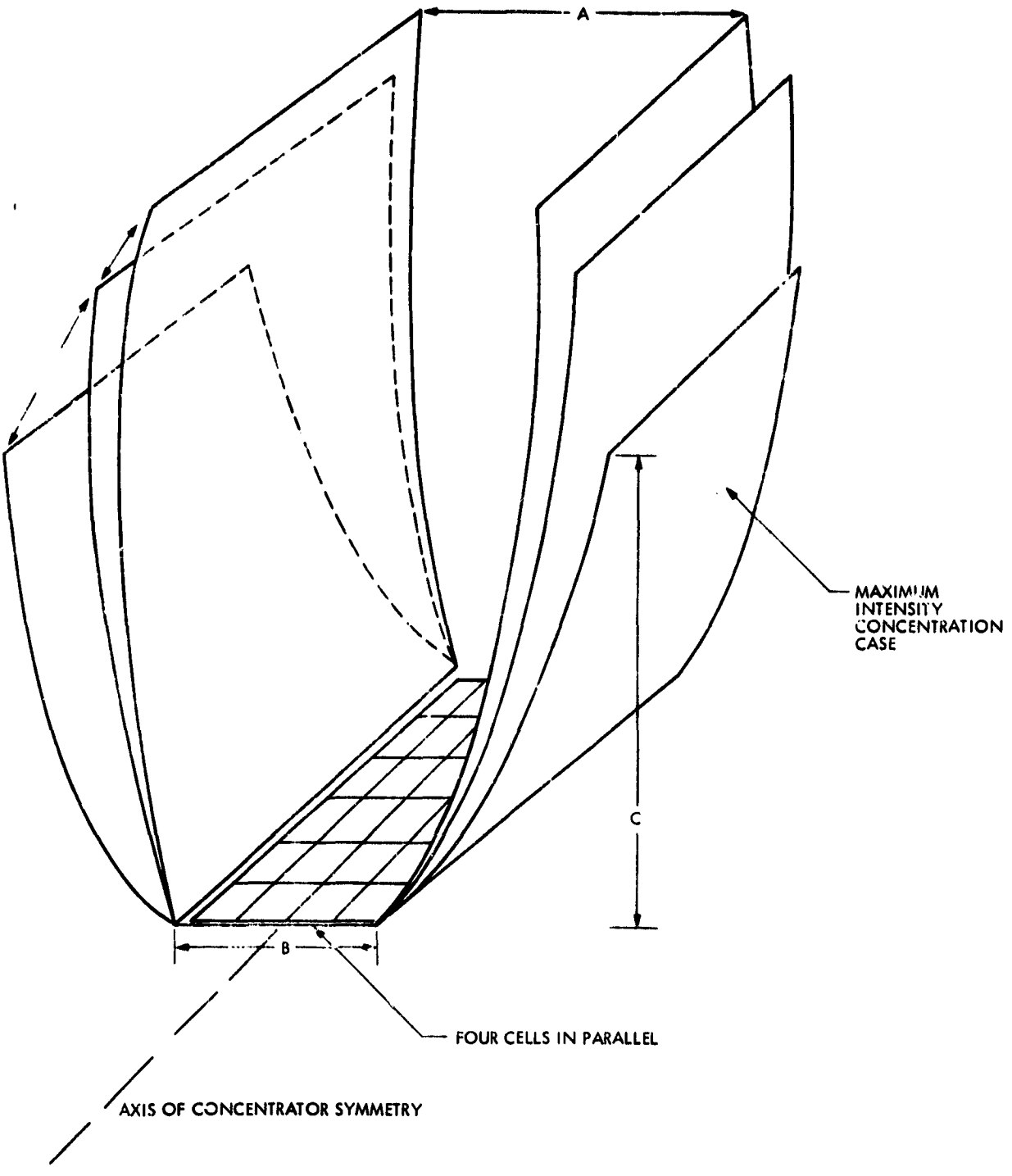

Figure 1. Compound Parabolic Concentrator (CPC) with Variable Intensity Concentration Ratio

CONCENTRATED INTENSITY DETERMINATION (RAY TRACE ROUTINE)

One thousand evenly spaced rays enter the CPC's entrance aperture and are traced until they encounter the array. With the CPC mirrors aligned in the maximum concentration configuration (Figure 2), all rays experience at most a single reflection before striking the array (assuming perfectly specular mirrors). As the concentration ratio (Cg) is decreased by tilting the tips of the mirrors inwards through an angle theta, multiple reflections are possible. However, all rays still reach the array. If mirror imperfections or intentionally stippled mirrors are considered (stippled mirrors are useful in reducing intensity nonuniformities), rays can be reflected back out the concentrator's entrance aperture. Such rays do not contribute to the generation of electrical power. The illustrative example deals exclusively with the specular mirror case.

The power per ray is determined from equation (1)

$$\text{Power of single ray} = \frac{\text{Total incident power entering concentrator's aperture over an arbitrary length along the axis of symmetry}}{\text{Total number of rays}} \qquad (1)$$

$$= \frac{IAC}{1000}$$

where I = incident intensity at concentrator's aperture (W/m^2)

A = width dimension of concentrator aperture (see Figure 1) (m)

C = arbitrary length along axis of symmetry (m)

The power per ray after a reflection is given by equation (2):

$$\text{Power (postreflection)} = \text{Power (prereflection)} \cdot (1-R) \qquad (2)$$

where R is the mirror reflectivity. (For a discussion of mirror reflectivity see Appendix A).

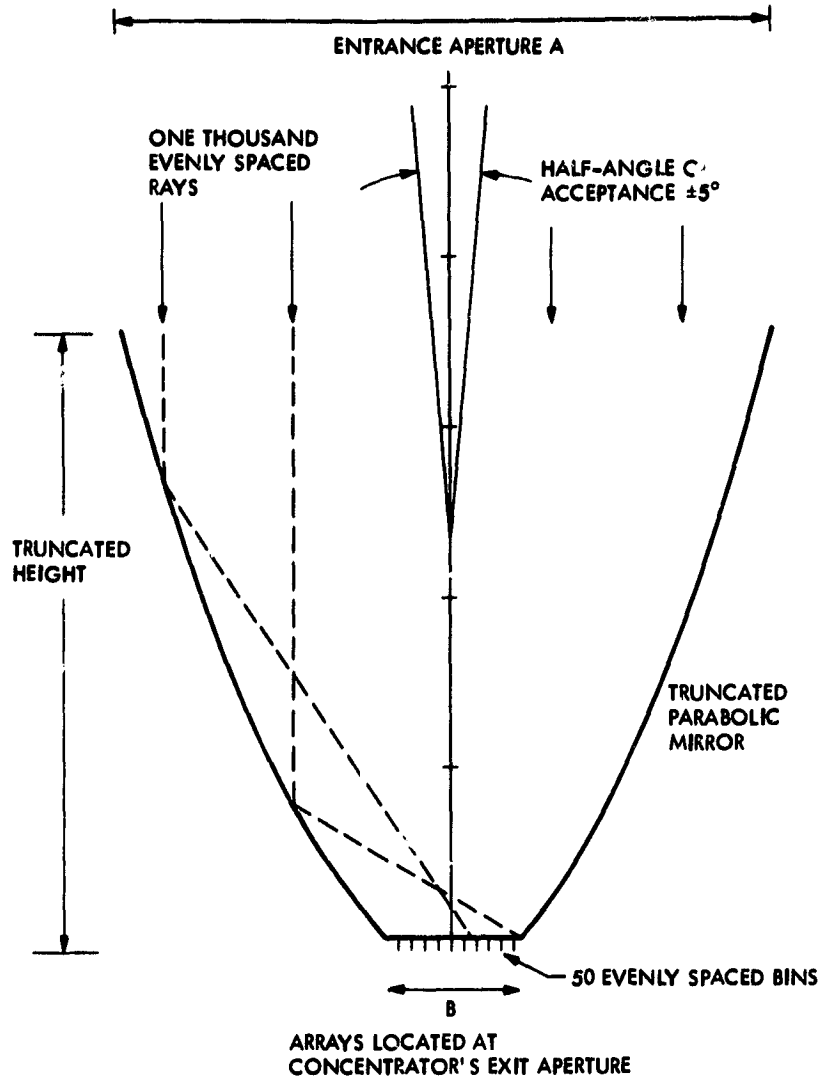

Figure 2. Typical Rays Traced through a CPC at the Maximum Concentration Configuration

The CPC exit aperture (colocated with the array) is divided into 50 bins for the purpose of counting rays. The incident power on each bin is the sum of the power of the incident rays. The intensity for each bin is the power per bin divided by the bin area [bin area = (B·C)/50]. B = width dimension of array (see Figure 1) (m). Note that the bin length (C) cancels itself in bin intensity and hence is an arbitrary value.

TABLE 1

Input Parameters for a Variable CPC Enhanced Array

θ (degrees)	Cg	Mirror height (cm)	"A" width (cm)	mirror reflectivity *
0	4.63	35.76	37.73	.865
1.9	4.34	36.23	35.34	.860
3.9	4.02	36.68	32.80	.860
6.0	3.69	37.11	30.90	.855
8.2	3.34	37.50	27.22	.850
10.3	3.00	37.83	24.46	.845
13.5	2.48	38.22	20.22	.850
17.9	1.76	38.58	14.31	.900

* see Appendix A

The first and the fiftieth bins are disregarded since cells are not positioned immediately next to the base of the mirrors. Rays entering these uncelled bins do not generate electrical power. The remaining 48 bins are assumed to overlay the 4 solar cells (see Figures 1 and 2). The intensities of the 12 bins overlaying each cell are averaged together to determine the average intensity reaching each solar cell. Table 1 shows how the geometric concentration ratio (Cg = A/B) and other parameters vary as the mirrors are tilted inwards through the theta angle measured from the maximum concentration configuration.

If the concentrator has a twist along the axis of symmetry, the intensity profile calculation must be repeated at various stations along the length of the concentrator. However, since this is not fundamentally more difficult, the no-twist case is illustrated.

The model also has the capability to introduce distortions into the mirrored surfaces. These can be either random in nature, simulating imperfections in specular surfaces, or periodic, simulating intentional mirror patterning, useful in reducing intensity nonuniformities. The illustrative example deals exclusively with the zero distortion, specular mirror case.

SOLAR CELL OPERATING TEMPERATURE DETERMINATION

Assuming that the solar cell is in good thermal contact with a substrate of known absorptivity and emissivity, the temperature of a solar cell operating in space can be calculated from Stefan's Law:

$$T^4 = \frac{(\alpha-\eta(T))S}{(\varepsilon_f+\varepsilon_b)\sigma} \qquad (3)$$

where

T = cell operating temperature (K)

α = absorptivity (dimensionless)

$\eta(T)$ = solar cell efficiency (itself a function of temperature and intensity) (dimensionless)

S = concentrated solar intensity (W/m^2)

ε_f = emissitivity of front surface (dimensionless)

ε_b = emissitivity of back surface (dimensionless)

σ = Stefan-Boltzmann Constant = $5.6696 \cdot 10^{-8}$ W/m^2 K^4

Since η, cell efficiency, is a function of temperature, it is necessary to assume an initial value of η and solve equation (1) by iteration. This iterative process converges rapidly but a computer based calculation avoids tiresome repetitive calculations and interpolations. Cell efficiency is interpolated from tabulated data as explained in the following section.

INDIVIDUAL CELL OUTPUT DETERMINATION

The individual cells short circuit current (Isc), maximum power current (Imp), open circuit voltage (Voc) and maximum power voltage (Vmp) are determined from tables of experimentally measured cell data (Reference 3). The tabular data set for each current and voltage is given between temperature and concentrated intensity limits of -160°C to 140°C and 5 mW/cm to 250 mW/cm, respectively. Data points are given at 20°C increments in temperature and at four intermediate intensities. Given an operating cell temperature and intensity, a linearly interpolated current or voltage is determined. Figures 3 and 4 show the respective variation of Voc and Vmp with intensity. While logarithmic interpolation is more appropriate than linear interpolation for voltages, the difference between the two interpolation methods typically amounts to less than 1 mV. This is well below the measured data standard deviation for either Voc or Vmp. Hence, the linear interpolation method was adopted for both current and voltage because it simplified the interpolation calculations with no meaningful loss in accuracy.

A limitation of the existing data is that the upper intensity limit of 250 mW/cm is exceeded for the illustrative example. The

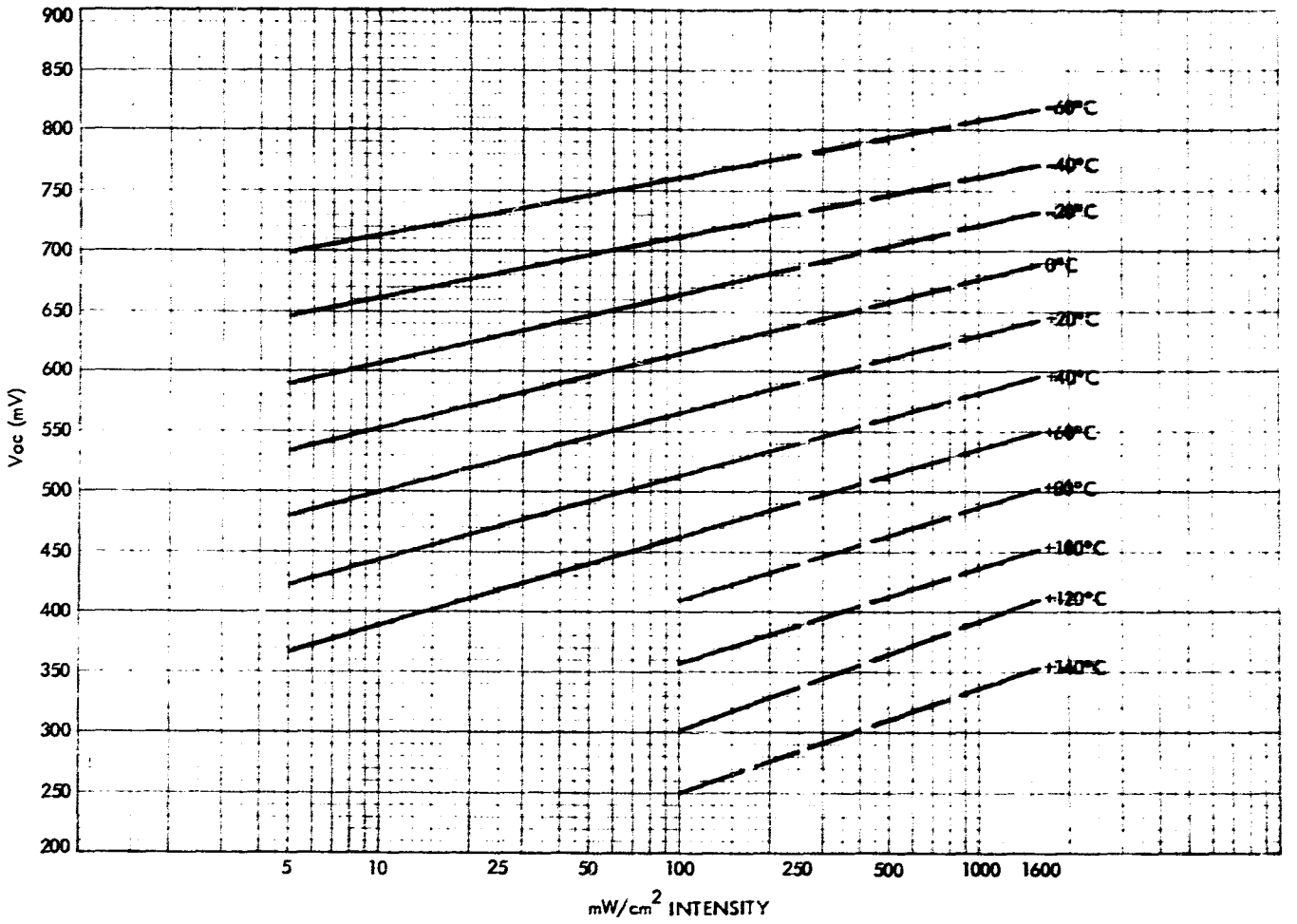

Figure 3. 2 x 2 cm Solarex 50 micron 2Ω -cm Voc (mV)

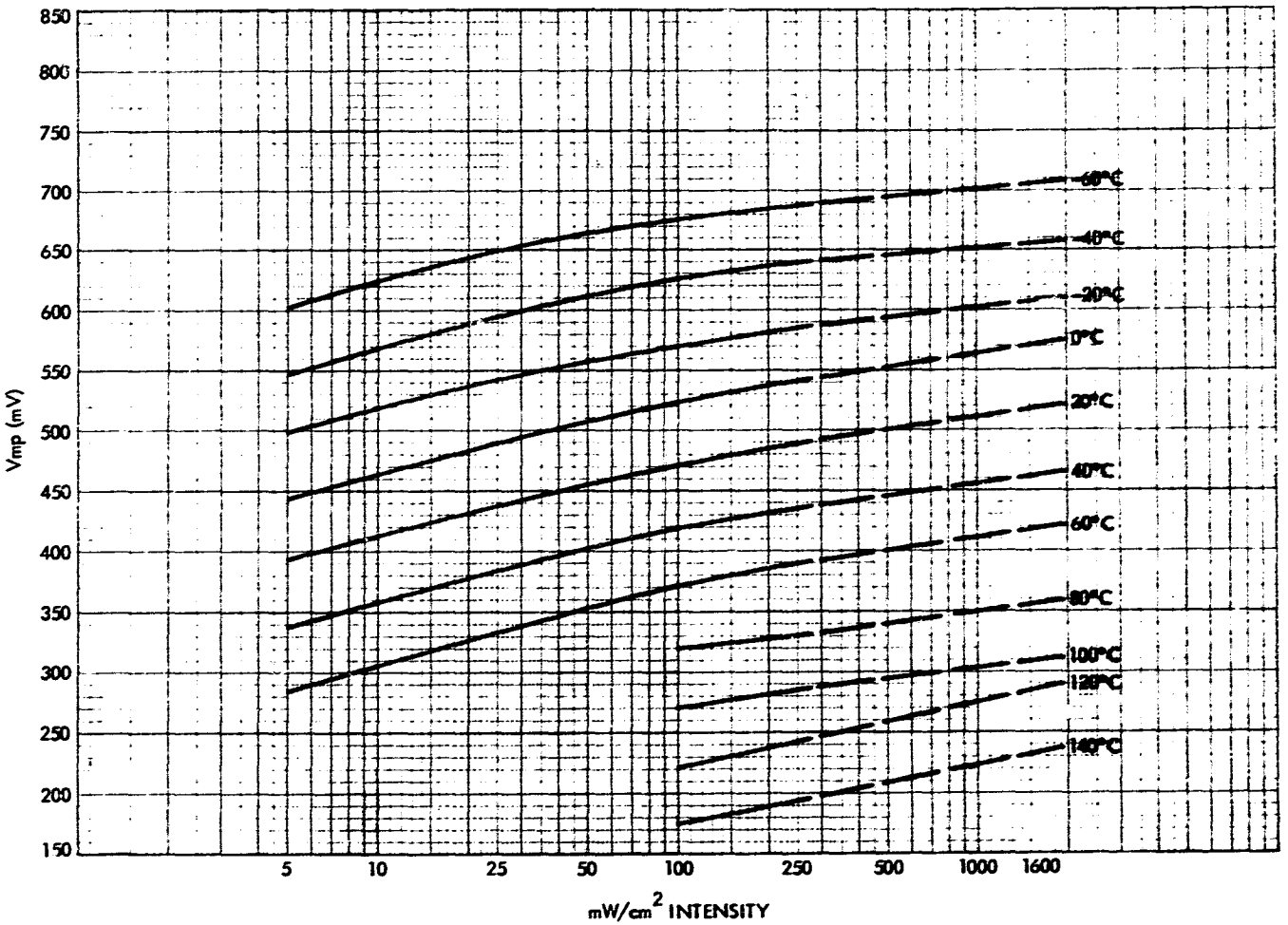

Figure 4. 2 x 2 cm Solarex Micron Vmp

existing data has been graphically extended to encompass these higher intensity regions (dashed lines of Figures 3 and 4). Experimental confirmation of these graphical extensions would be highly desirable.

PARALLELED CELL STRING OUTPUT DETERMINATION

Paralleled cells in a compound parabolic concentrator enhanced array experience widely different temperature/intensity conditions. Localized intensities of over 1250 mW/cm^2 (over 9 suns) at an incident intensity of 67.65 mW/cm^2 (half sun) are predicted. Under these conditions, localized temperature hot spots reach 275°C. The resulting cell's current and voltage outputs also vary widely. Similar, though less extreme variations, can be caused by inherent cell-to-cell differences. The resulting mismatches in cell powers reduces the total available power below that of the simple sum of individual cell powers. The single diode model of a solar cell is used to predict the output of the mismatched paralleled cells. This technique essentially generates an I-V curve for each paralleled cell. The single diode model parameters for each cell are adjusted so that they agree with the Isc, Imp, Voc, Vmp, and series resistance (R_s) values of each cell in the parallel string. Once the single diode model parameters are made to match the observed values of each cell, then the cell's entire I-V curve is uniquely specified. The individual cell's I-V curves may then be algebraically added to give the total paralleled string I-V performance curve. From this curve, the string's outputed power is easily determined (Reference 4).

The equations necessary to determine the individual cell I-V curves will now be derived from the basic single diode equivalent circuit for a solar cell, which follows:

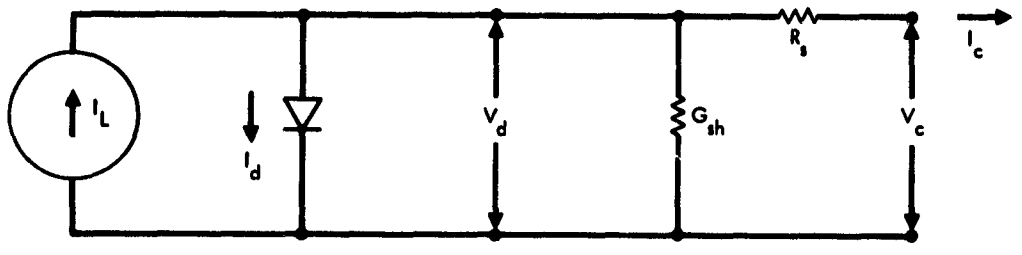

WHERE I_L IS A CONSTANT CURRENT GENERATOR

Let:

I_c = load current
V_c = load voltage
I_o = reverse saturation current
I_L = light generated current (a constant current generator)
G_{sh} = shunt conductance (an initial estimate provides for faster convergence but is not required)
I_d = diode current
$E_o = \frac{AkT}{q}$
A = an assumed constant
k = Boltzmann constant
T = temperature (K)
q = electron charge
R_s = series resistance
Isc = short circuit current
Imp = maximum power current
Voc = open circuit voltage
Vmp = maximum power voltage
Pmax = Imp · Vmp = maximum power

From the basic diode equation:

$$I_L = I_o \left[\exp\left(\frac{V_c + I_c R_s}{E_o}\right) - 1\right] + (V_c + I_c R_s) G_{sh} + I_c \qquad (4)$$

Evaluating (2) at the short and open circuit conditions one obtains respectively:

$$I_L = I_o \left[\exp\left(\frac{Isc\ R_s}{E_o}\right) - 1\right] + Isc\ (1 + R_s G_{sh}) \qquad (5)$$

and

$$I_L = I_o \left[\exp\left(\frac{Voc}{E_o}\right) - 1\right] + Voc\ G_{sh} \qquad (6)$$

At the maximum power point

$$I_L = I_o \left[\exp \left(\frac{Vmp + Imp\ R_s}{E_o}\right) - 1 \right] + Vmp\ G_{sh} + Imp\ (1 + R_s\ G_{sh}) \qquad (7)$$

also since $\frac{dP}{dV} = 0$ at the maximum power point;

$$-\frac{Imp}{Vmp} = \left.\frac{dI_c}{dV_c}\right|_{V_c = Vmp} \qquad (8)$$

differentiating (2) with respect to V_c and using (6), one obtains:

$$\frac{Imp}{Vmp} = \frac{G_{sh} + \frac{I_o}{E_o} \exp \left(\frac{Vmp + Imp\ R_s}{E_o}\right)}{1 + R_s\ G_{sh} + \frac{I_o\ R_s}{E_o} \exp \left(\frac{Vmp + Imp\ R_s}{E_o}\right)} \qquad (9)$$

Using (3), (4), (5) and (7) to eliminate I_L, G_{sh}, and I_o, one obtains;

$$E_o = \frac{(Vmp - Imp\ R_s)\ (Voc - Isc\ R_s)\ (Isc\ Vmp - Isc\ Voc + Imp\ Voc)}{\frac{X_o}{X_m} Vmp\ (Voc - Isc\ R_s)(2Imp - Isc) - (Voc - Isc\ R_s)(Imp\ Voc - Isc\ Vmp) - \frac{X_s}{X_m} Imp(2Vmp - Voc)(Voc - Isc\ R_s)} \qquad (10)$$

where

$$X_s = \exp \left(\frac{Isc\ R_s}{E_o}\right);\ X_o = \exp \left(\frac{Voc}{E_o}\right);\ X_m = \exp \left(\frac{Vmp + Imp\ R_s}{E_o}\right)$$

Equation (10) is solvable by iteration.

Once E_o is known then I_o and G_{sh} are obtained from:

$$I_o = \frac{Isc\ Vmp - Isc\ Voc + Imp\ Voc}{(X_o - X_s)\ (Vmp + Imp\ R_s) - (X_m - X_s)\ Voc - Isc\ R_s\ (X_o - X_m)}$$

and

$$G_{sh} = \frac{Isc - I_o\ (X_o - X_s)}{Voc - Isc\ R_s}$$

I_L is then obtained from (4); I_c as a function of V_c is then obtained (i.e. the I-V curve is obtained). In this manner, the I_c of each paralleled cell can be calculated for every V_c. Summing the individual cell I_c values for given values of V_c yields the total paralleled string I-V curve.

ARRAY OUTPUT DETERMINATION

As currently configured, the model assumes that the array consists of a single circuit. The model can be generalized to an array consisting of an arbitrary set of n circuits. As configured, the I-V curve for the circuit is the algebraic sum of the paralleled string curves.

Table 2 summarizes the Appendix B results for the variable concentration CPC enhanced thin cell array with specular mirrors. The theta angle is the angle the mirrors have been tilted inwards from the maximum geometric intensity design point. The figure of merit W shown in the last column of Table 2 indicates the power gain of the concentrator enhanced thin cell array as referenced to an identical unconcentrated thin cell array (identical thermal properties) operating under identical incident intensity conditions (see Fig. 5).

TABLE 2

Summary of Appendix B Results for the
Variable CPC Thin Cell Array with Specular Mirrors*

mirror angle Θ (degrees)**	geometric intensity concentration ratio	predicted 80 cell array module output			"W"
		voltage(V) Vmp	amperage(A) Imp	power(W) PMP	
0.0	4.629	2.200	.804	1.769	.66
1.9	4.336	2.600	.808	2.100	.79
3.9	4.024	4.000	.792	3.166	1.19
6.0	3.692	5.600	.752	4.209	1.58
8.2	3.340	6.400	.711	4.551	1.71
10.3	3.002	6.000	.615	3.692	1.38
13.5	2.480	6.200	.506	3.138	1.18
17.9	1.756	7.800	.397	3.094	1.16

*Assumptions as follows: 80 cell module, 2x2 cm cells, 4 cells in parallel spread across width of the CPC; incident unconcentrated intensity 67.65 mW/cm^2; array thermal absorptivity = 0.84, array front hemispherical emissitivity = 0.83, array back hemispherical emissitivity = 0.76; cell series resistance = .2 ohms.

**Mirror angle referenced to the maximum geometric intensity concentration design point.

Figure 5 is a smoothed graphical representation of Table 2.

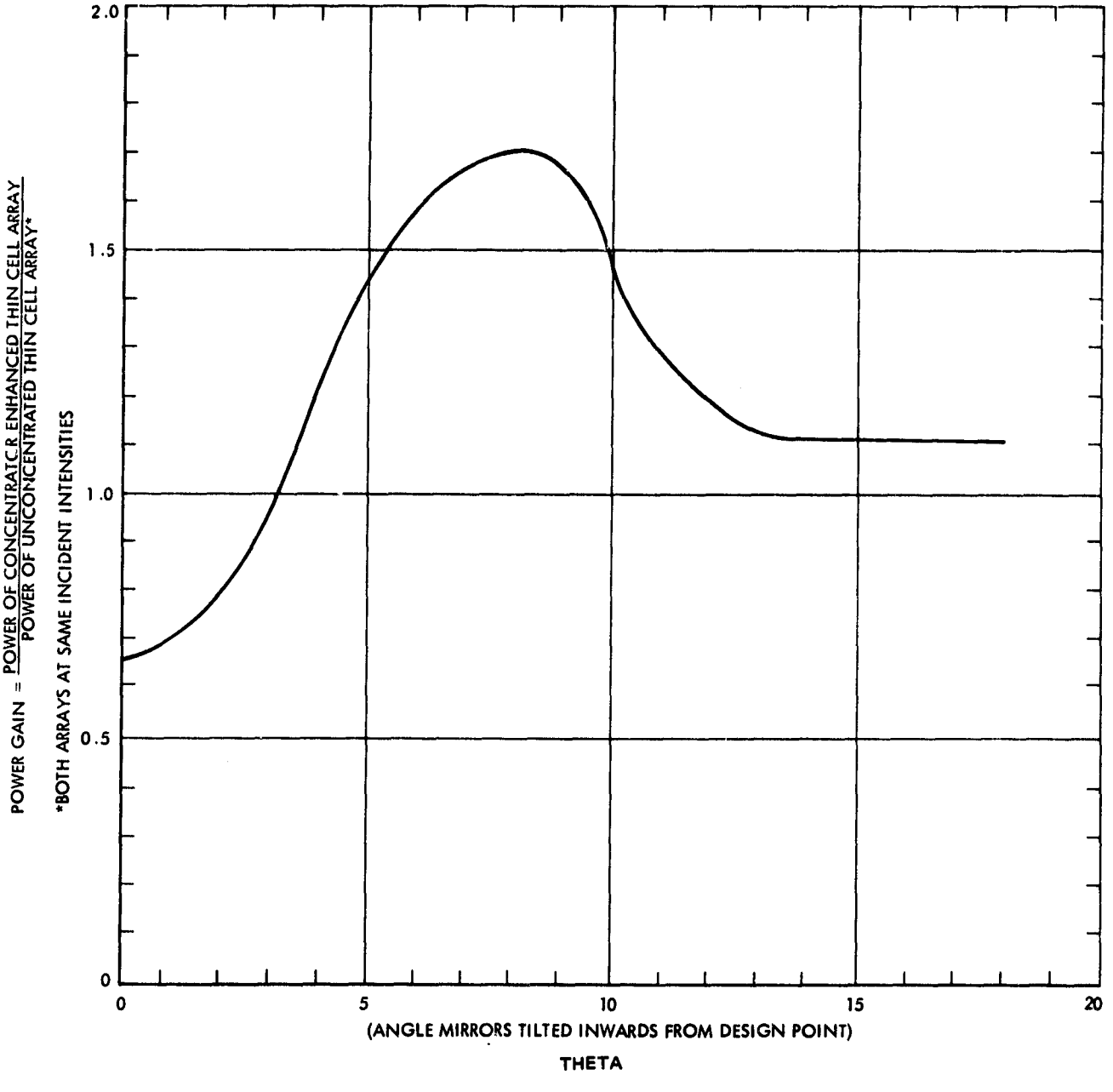

Figure 5. The CPC Power Gain (W) vs Mirror Angle Tilt

SUMMARY OF RESULTS FOR THE ILLUSTRATIVE EXAMPLE

The CPC enhanced thin cell array with specular mirrors does not generate its peak power at the maximum intensity design point. The dominant cause is that the specular CPC is plagued by nonuniform intensity patterns which produce localized intensities as high as 1250 mW/cm^2 (over 9 suns) at an incident intensity of 67.65 mW/cm^2. These nonuniformities result in localized hot spots which reach 275°C. Maximum power was generated with the mirrors angled inwards 8.2 degrees from the maximum intensity design point. While this concentrator design is almost certainly not the optimal design for this operating environment, the power gain as referenced to an unconcentrated array, operating under similar incident intensity conditions, is a factor of 1.7. Whether such a power gain is sufficient to pay back the added cost, mass, and complexity of the concentrator system remains an open question.

CONCLUSION

The general computer modeling approach developed in this memo provides a method for predicting the power output, uniformity of intensity, and operating temperature of a concentrator enhanced solar array. This modeling technique can be used to evaluate the relative merits of various concentrator concepts. Based upon the results of additional modeling, candidate concepts can be proposed for scale model testing.

ACKNOWLEDGMENT

The author gratefully acknowledges programmming and data run support provided by Zoltan Uzdy of the general purpose computing services section.

REFERENCES

1. Final Phase I Report: "Winston Solar Concentrators and Evaluation Support," The Enrico Fermi Institute, the University of Chicago, JPL Contract 954563, September 1977.

2. Final Phase II Report: "Non-Imaging Concentrators for Space Applications," The Enrico Fermi Institute, The University of Chicago, JPL Contract 954563, August 28, 1978.

3. Characterization of Solar Cells for Space Applications, Publication 78-15, Vol. II, R. G. Downing, T. F. Miyahira, R. S. Weiss, August 15, 1978. Jet Propulsion Laboratory, Pasadena, Calif.

4. IOM #341-78-A-191, T. Koerner, "Computer Model for Solar Cell," August 21, 1978. Jet Propulsion Laboratory, Pasadena, Calif. (JPL internal document.)

APPENDIX A

REFLECTIVITY MODEL FOR MIRRORED SURFACES

APPENDIX A: Reflectivity Model for Mirrored Surfaces

The current model provides mirror reflectivity as a function of angle of incidence.

TABLE A-1. Mirror Reflectivity vs Angle of Incidence

angle of incidence (degrees)	mirror reflectivity
0 (normal to mirror surface)	.90
5	.90
10	.90
15	.90
20	.90
25	.90
30	.89
35	.89
40	.89
45	.89
50	.89
55	.88
60	.88
65	.87
70	.86
75	.85
80	.84
85	.87
90	1.00

The "angle of incidence" here refers to the angle an incident ray makes to the plane connecting the extreme inboard and outboard edges of the mirror. While a single value of reflectivity does not allow for the changing angle of incidence along the curvature of the mirror, it does represent an "average" value of reflectivity.

Reflectivity values are based upon information supplied by Dr. B. Zeldin. Dr. Zeldin supplied a matrix of reflectivity values for an aluminized mirror at a specific wavelength and a specific angle of incidence (see Appendix A: Table A-2). A single value of reflectivity for each angle of incidence is obtained by weighting the reflectivity at a particular wavelength by the amount of energy present in the solar spectrum at that particular wavelength. Table A-3 of Appendix A contains the weighting factors for each wavelength. The final result is the angle dependent reflectivity shown in Appendix A, Table A-1.

TABLE A-2. Estimates of Reflectivity of Mirrored Surfaces as a Function of Angle of Incidence and Waveguide (Supplied by Dr. B. Zeldin in private communication)

Wave-Length (A)	ANGLE OF INCIDENCE (DEGREES)																		
	0	5	10	15	20	25	30	35	40	45	50	55	60	65	70	75	80	85	90
4000	.91	.91	.91	.91	.91	.91	.91	.91	.91	.90	.90	.90	.90	.89	.89	.89	.90	.94	1.00
4500	.91	.91	.91	.91	.91	.91	.91	.90	.90	.90	.90	.90	.89	.89	.88	.88	.89	.92	1.00
5000	.90	.90	.90	.90	.90	.90	.90	.90	.90	.90	.90	.89	.89	.88	.87	.87	.88	.91	1.00
5500	.90	.90	.90	.90	.90	.90	.90	.90	.90	.90	.90	.89	.89	.88	.87	.87	.86	.90	1.00
6000	.90	.90	.90	.90	.90	.90	.90	.90	.90	.90	.90	.89	.89	.88	.87	.86	.85	.88	1.00
6500	.90	.90	.90	.90	.90	.90	.90	.90	.90	.89	.89	.89	.88	.87	.86	.85	.83	.85	1.00
7000	.89	.89	.89	.89	.89	.89	.89	.89	.89	.88	.88	.88	.87	.86	.85	.83	.81	.83	1.00
7500	.88	.88	.88	.88	.88	.88	.88	.88	.87	.87	.87	.86	.86	.85	.83	.81	.80	.81	1.00
8000	.87	.87	.87	.87	.87	.87	.87	.87	.87	.87	.86	.86	.85	.84	.82	.80	.79	.80	1.00
8500	.86	.86	.86	.86	.86	.86	.86	.86	.86	.86	.85	.85	.84	.83	.81	.79	.77	.79	1.00
9000	.88	.88	.88	.88	.88	.88	.88	.88	.88	.88	.88	.87	.86	.85	.84	.82	.80	.81	1.00
9500	.91	.91	.91	.91	.91	.91	.91	.91	.91	.91	.91	.90	.90	.89	.87	.86	.83	.83	1.00

TABLE A-3. Weighting Factor for Mirror Reflectivity vs. Wavelength

Wavelength (Å)	Weighting Factor
4000	.71
4500	1.00
5000	.97
5500	.86
6000	.83
6500	.76
7000	.68
7500	.62
8000	.55
8500	.50
9000	.44
9500	.41

APPENDIX B

RESULTS OF THE VARIABLE CPC WITH SPECULAR MIRRORS IN COMBINATION WITH THE 50-MICRON SOLAREX CELL

Appendix B contains a graphical summary of the intensity, temperature and I-V curve results for each mirror tilt angle. Each of the temperature and intensity plots gives a graphical representation of temperature and intensity variation across the array width. The I-V graphs show three I-V curves per graph. The lower curves are individual cell curves while the upper curve is the algebraic sum of the individual cell curves. Only two of the four individual cell curves need be considered since the other two possess identical characteristics because of concentrator symmetry. Some of the I-V curves have been truncated by computer limitations, however, the curves still demonstrate the circuit effect of intensity/ temperature induced cell mismatches.

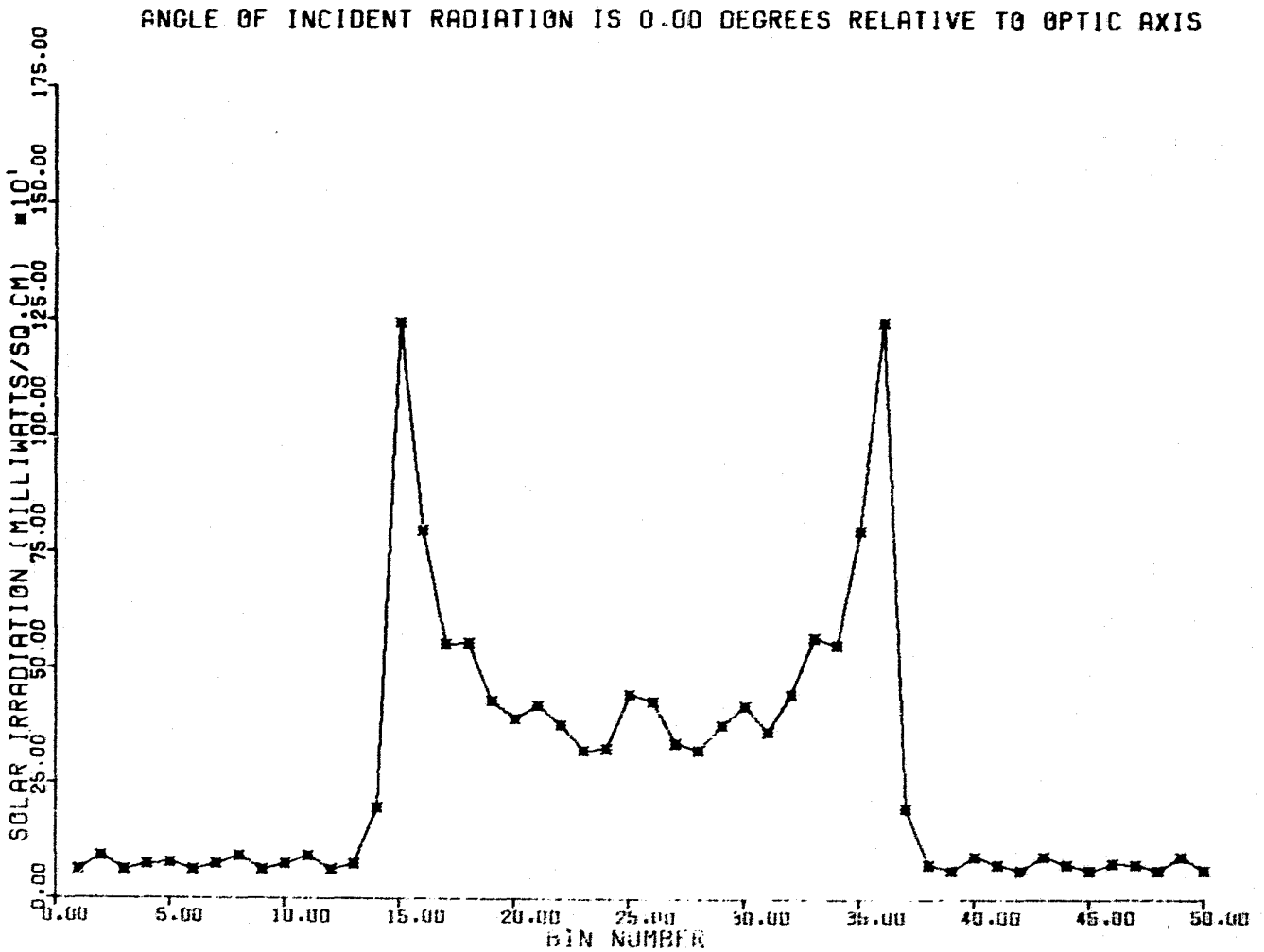

Figure B-1. Intensity vs Bin No. for Theta = 0.0 deg Configuration

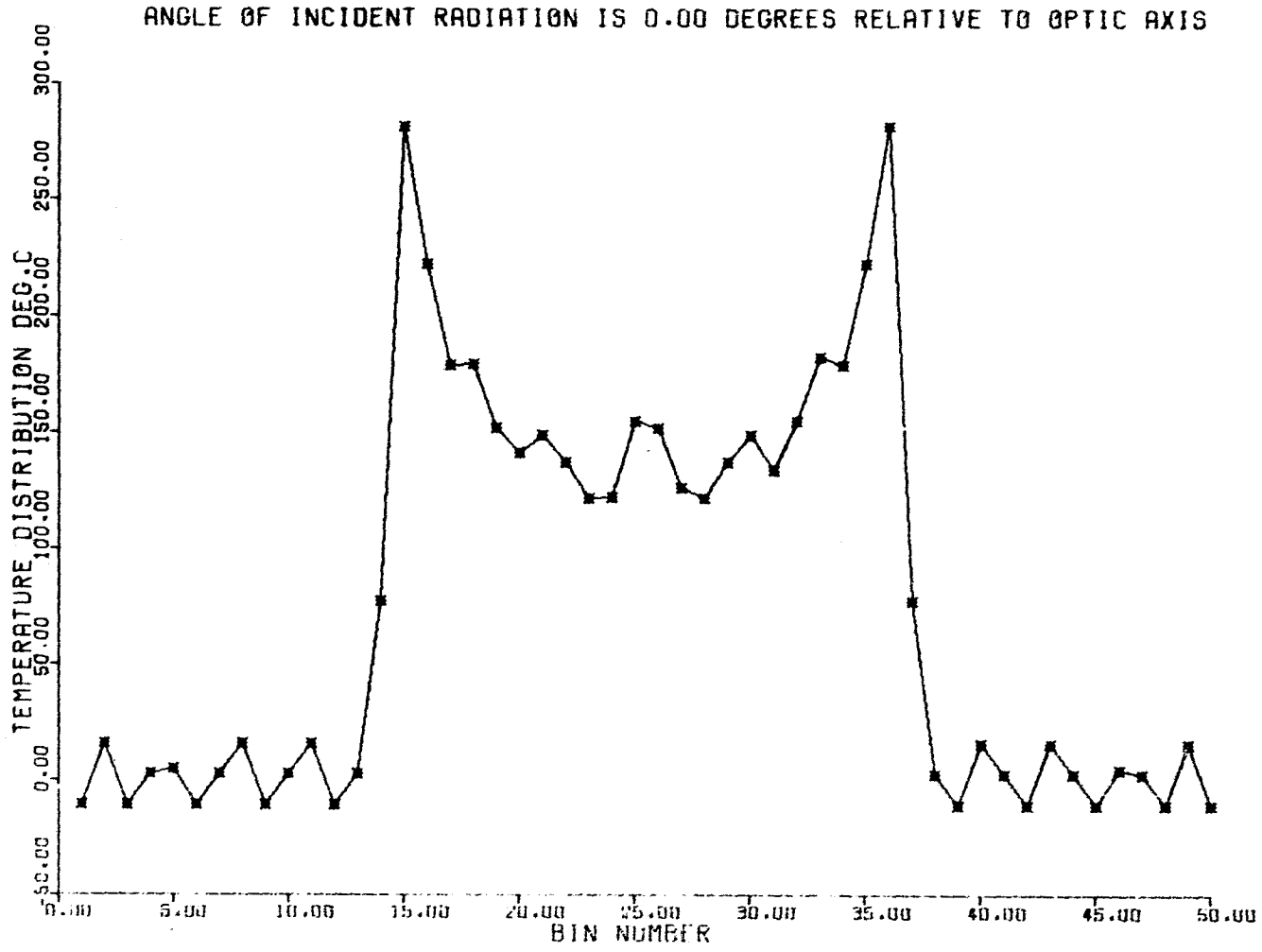

Figure B-2. Temperature vs Bin No. for Theta = 0.0 deg Configuration

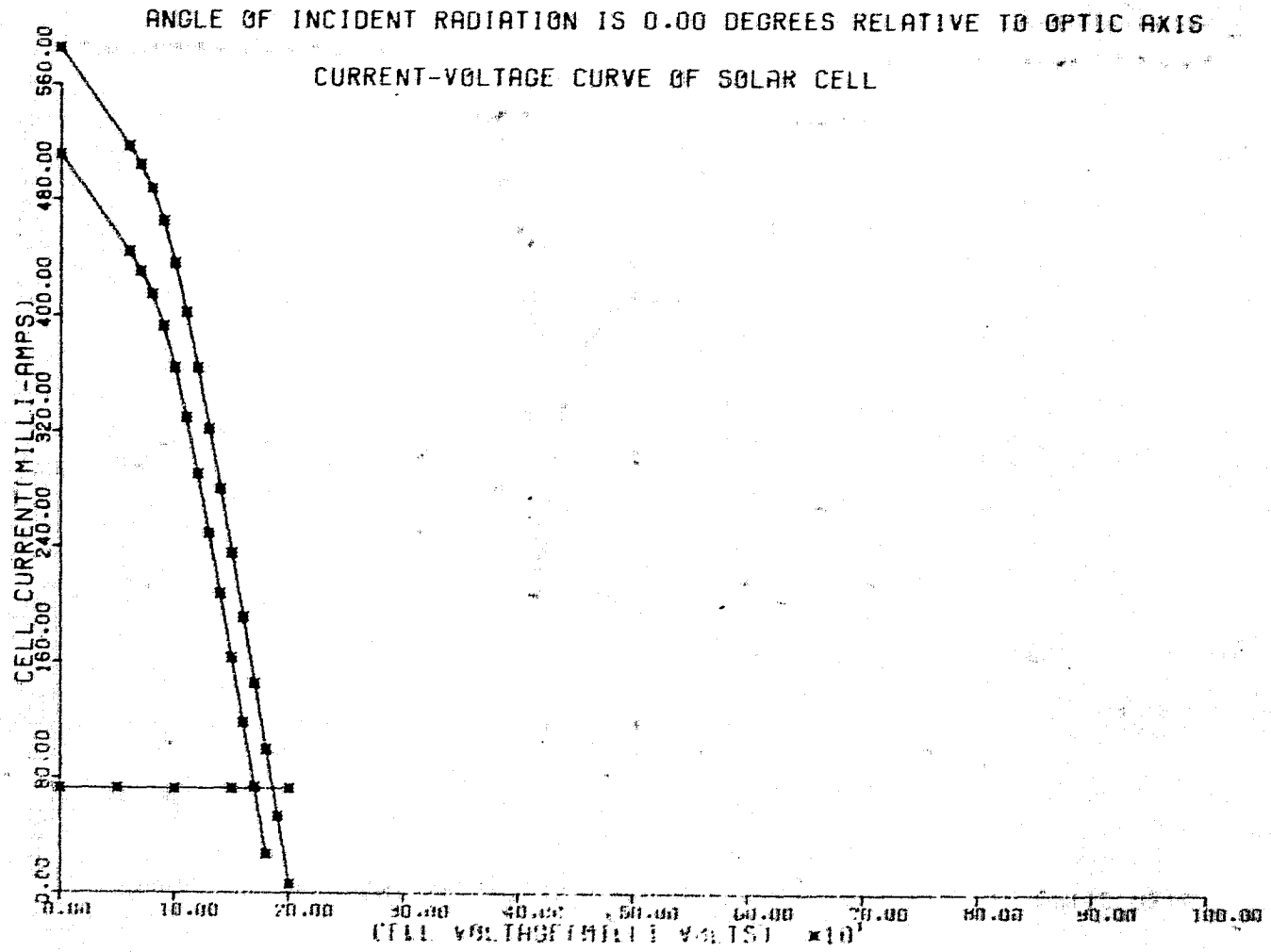

Figure B-3. Array I-V Curve for Theta = 0.0 deg

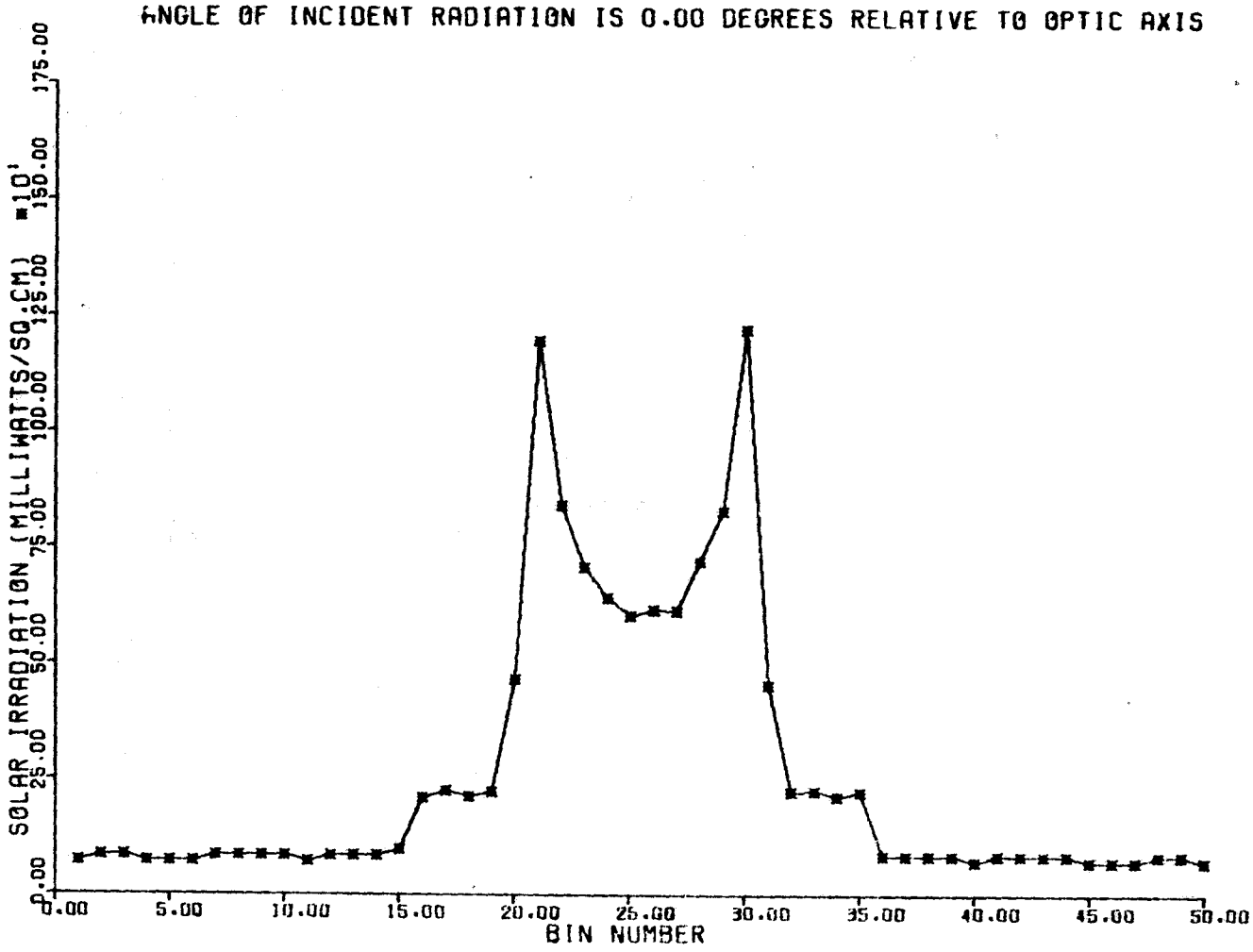

Figure B-4. Intensity vs Bin No. for Theta = 1.9 deg Configuration

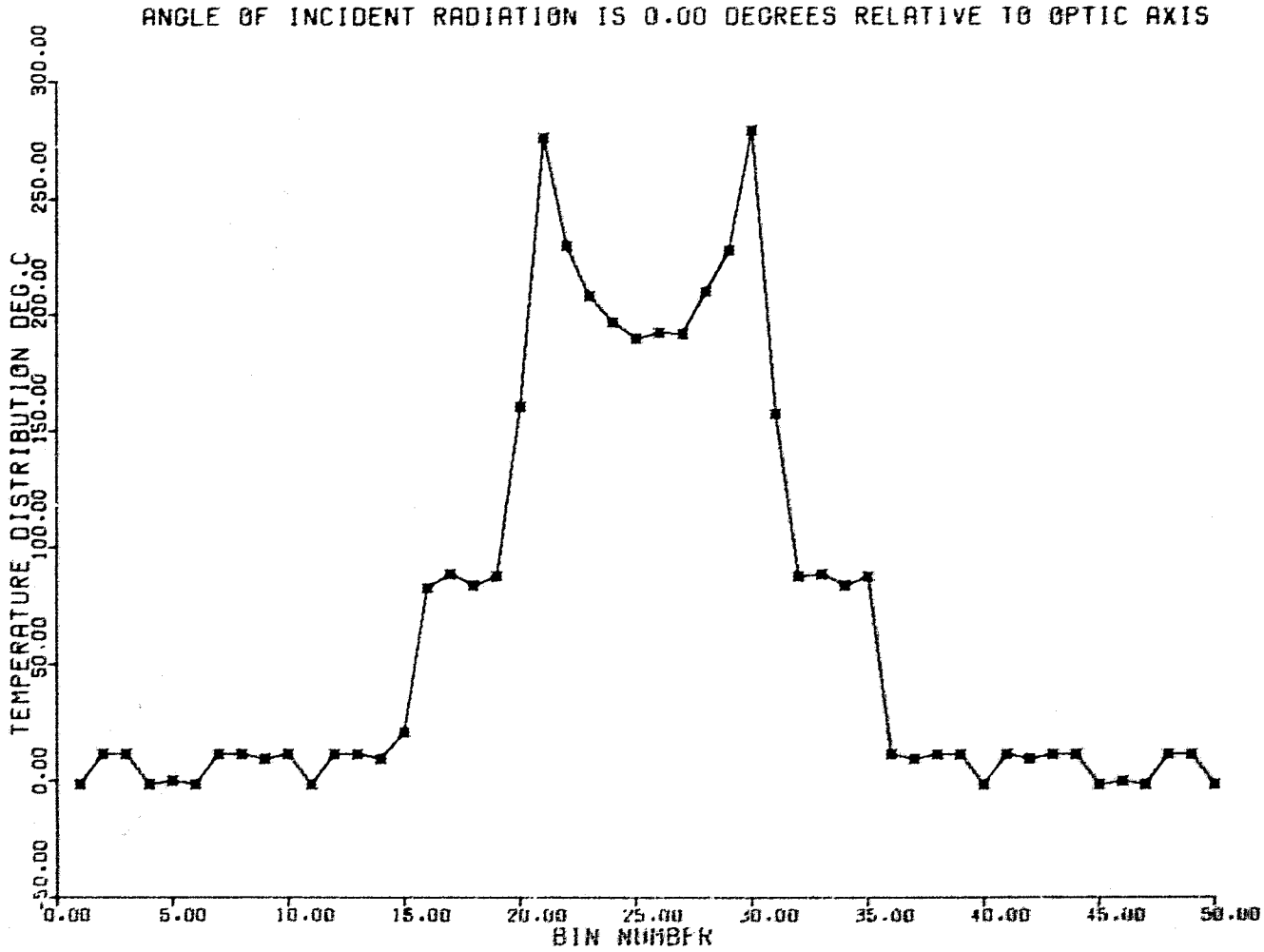

Figure B-5. Temperature vs Bin No. for Theta = 1.9 deg Configuration

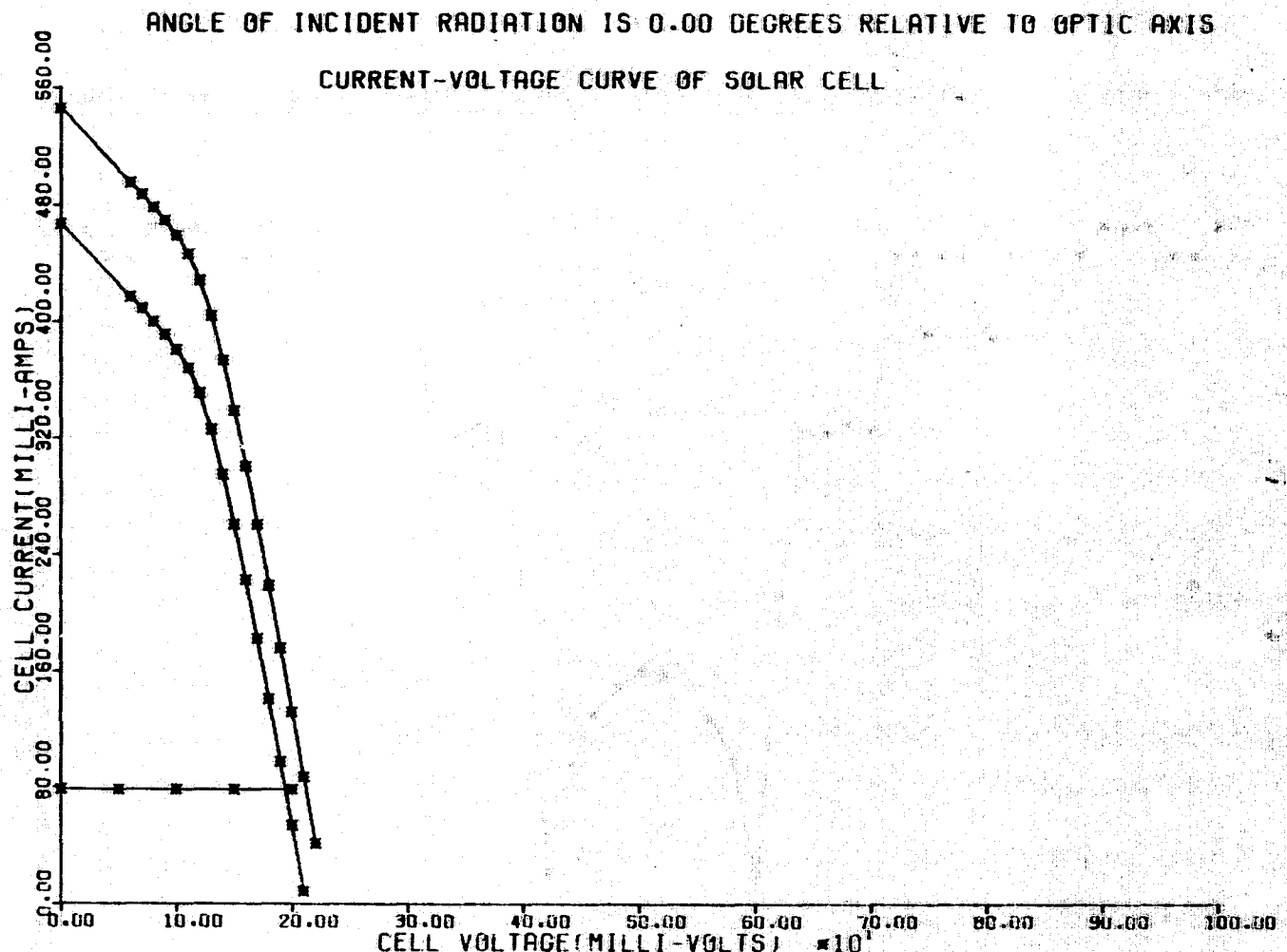

Figure B-6. Array I-V Curve for Theta = 1.9 deg

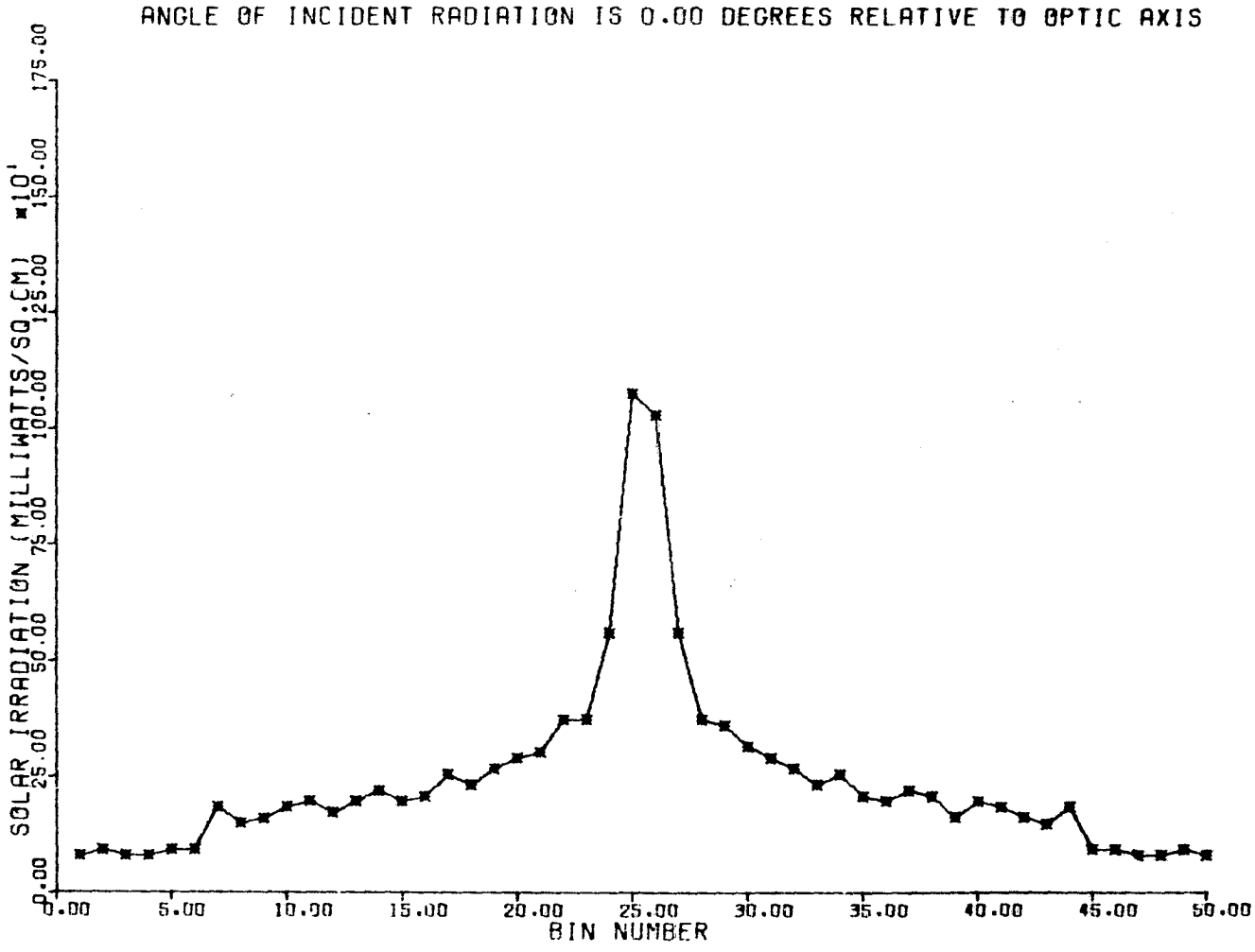

Figure B-7. Intensity vs Bin No. for Theta = 3.9 deg Configuration

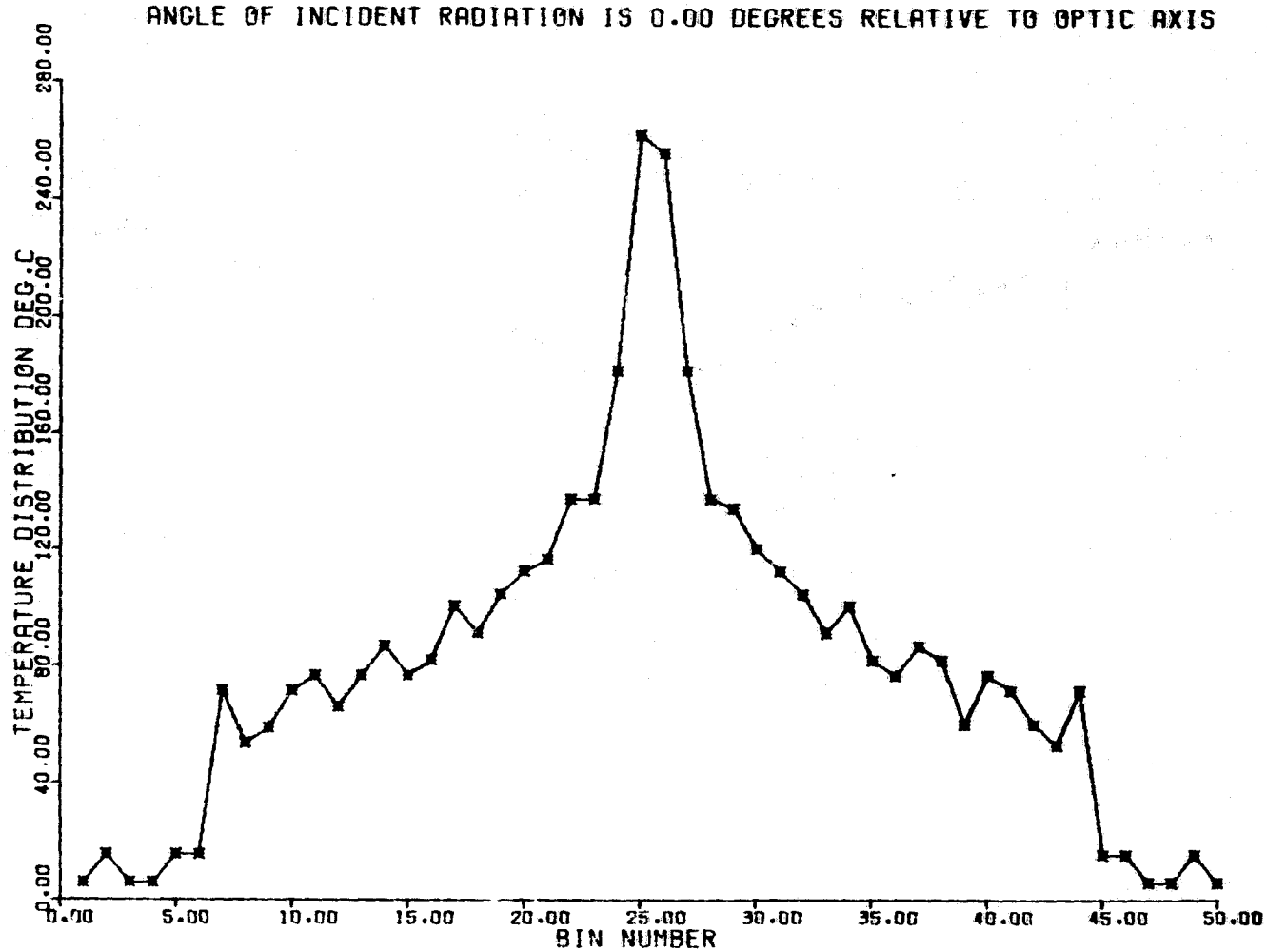

Figure B-8. Temperature vs Bin No. for Theta = 3.9 deg Configuration

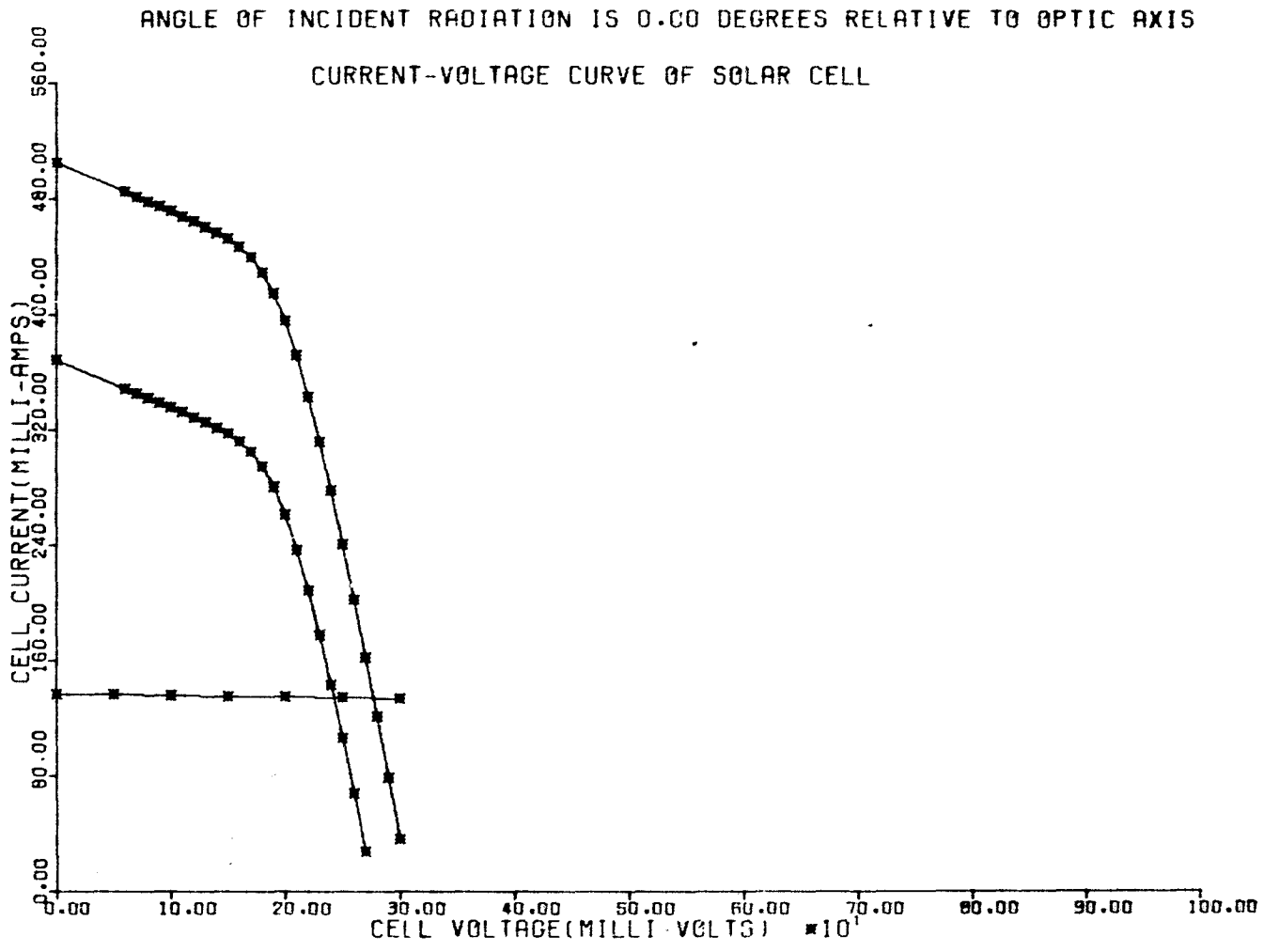

Figure B-9. Array I-V Curve for Theta = 3.9 deg

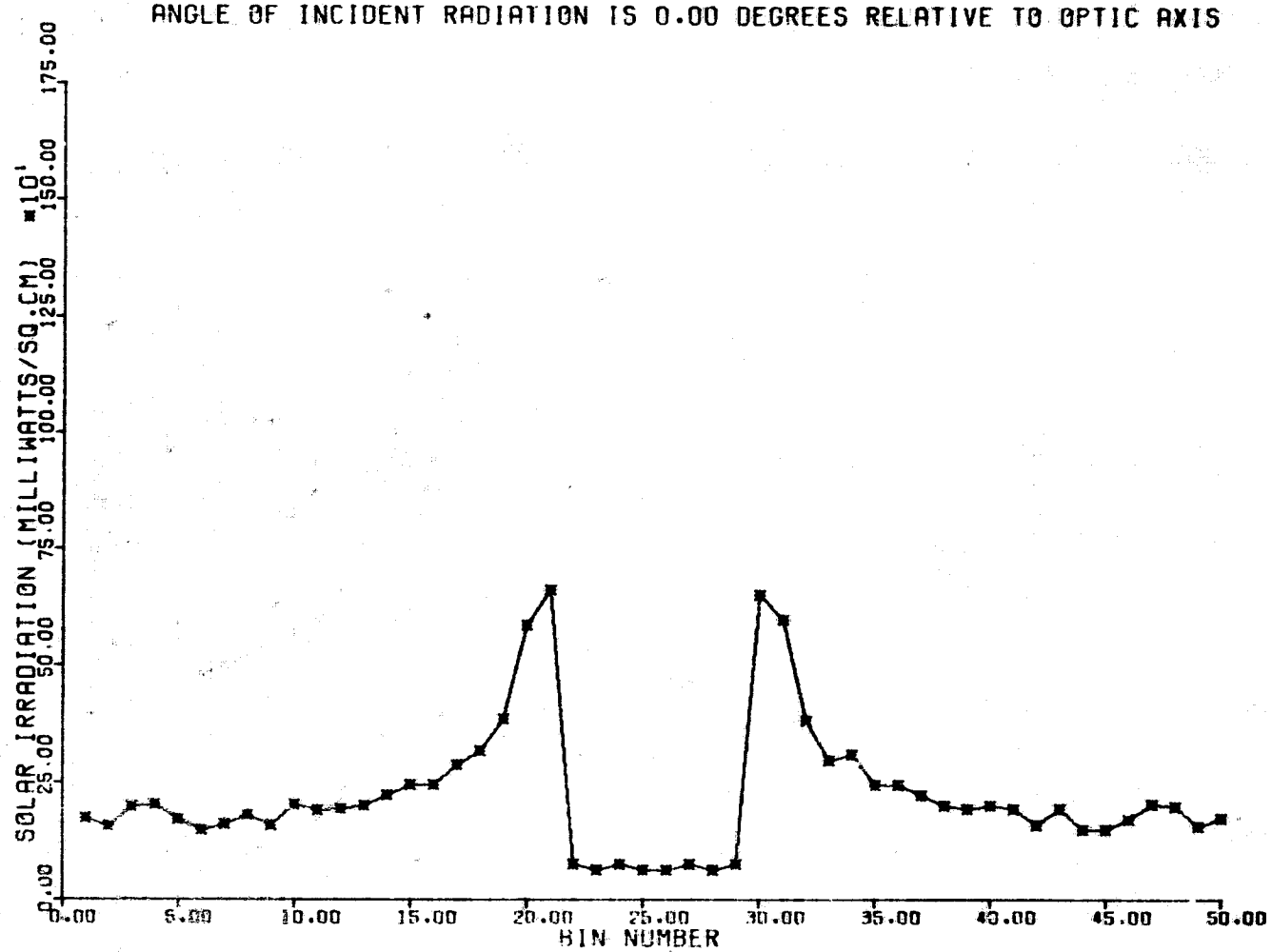

Figure B-10. Intensity vs Bin No. for Theta = 6.0 deg Configuration

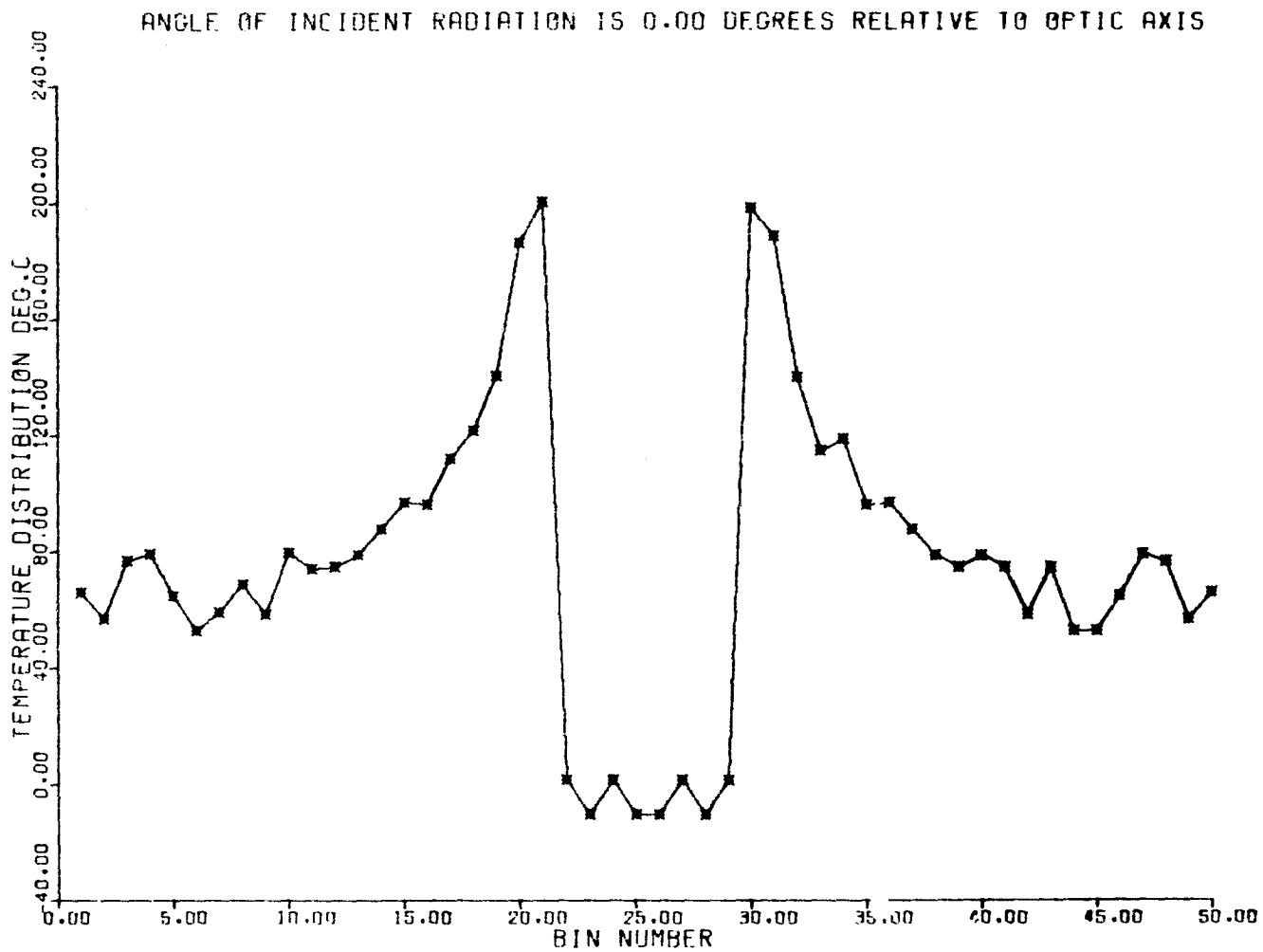

Figure B-11. Temperature vs Bin No. for Theta = 6.0 deg Configuration

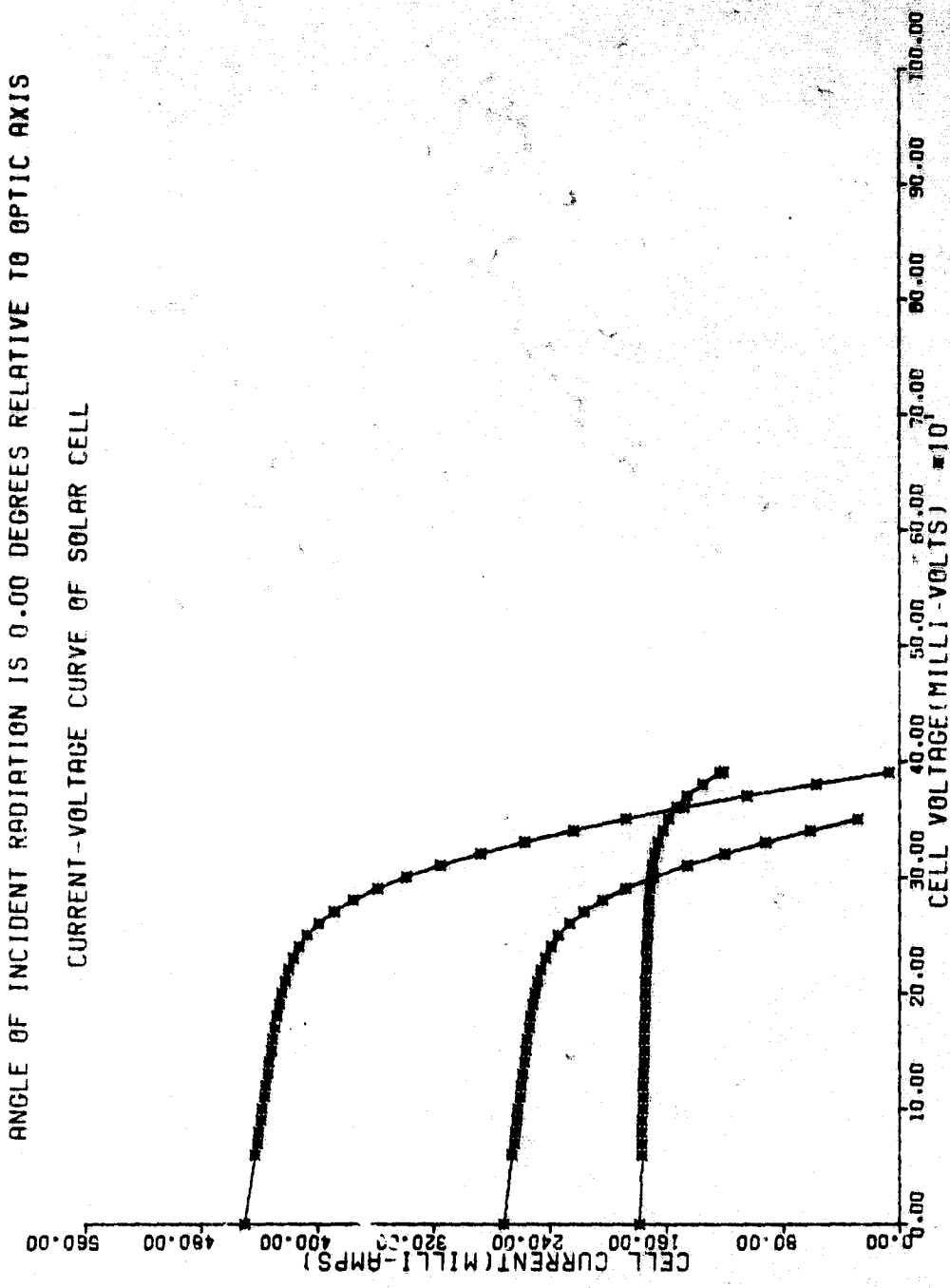

Figure B-12. Array I-V Curve for Theta = 6.0 deg

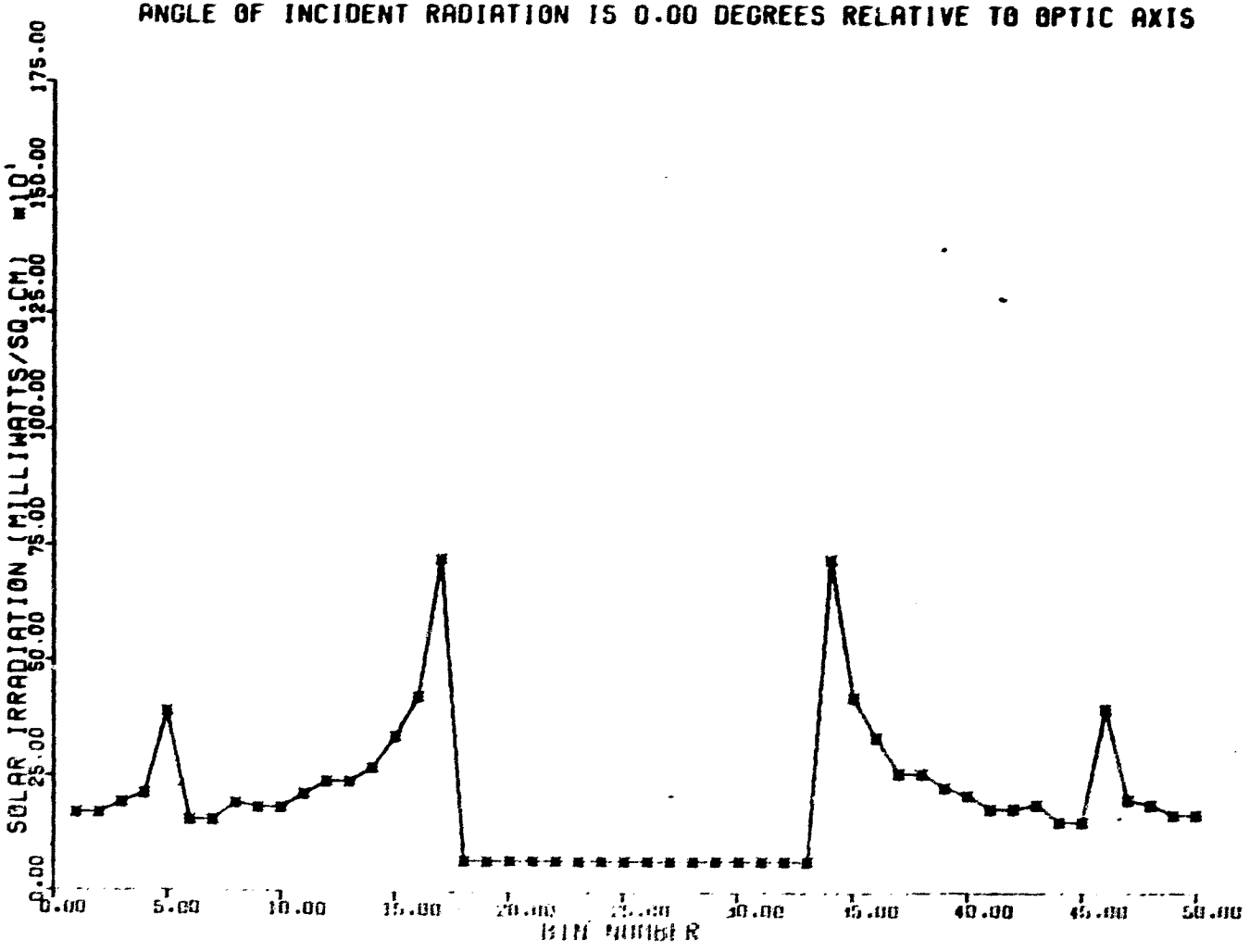

Figure B-13. Intensity vs Bin No. for Theta = 8.2 deg Configuration

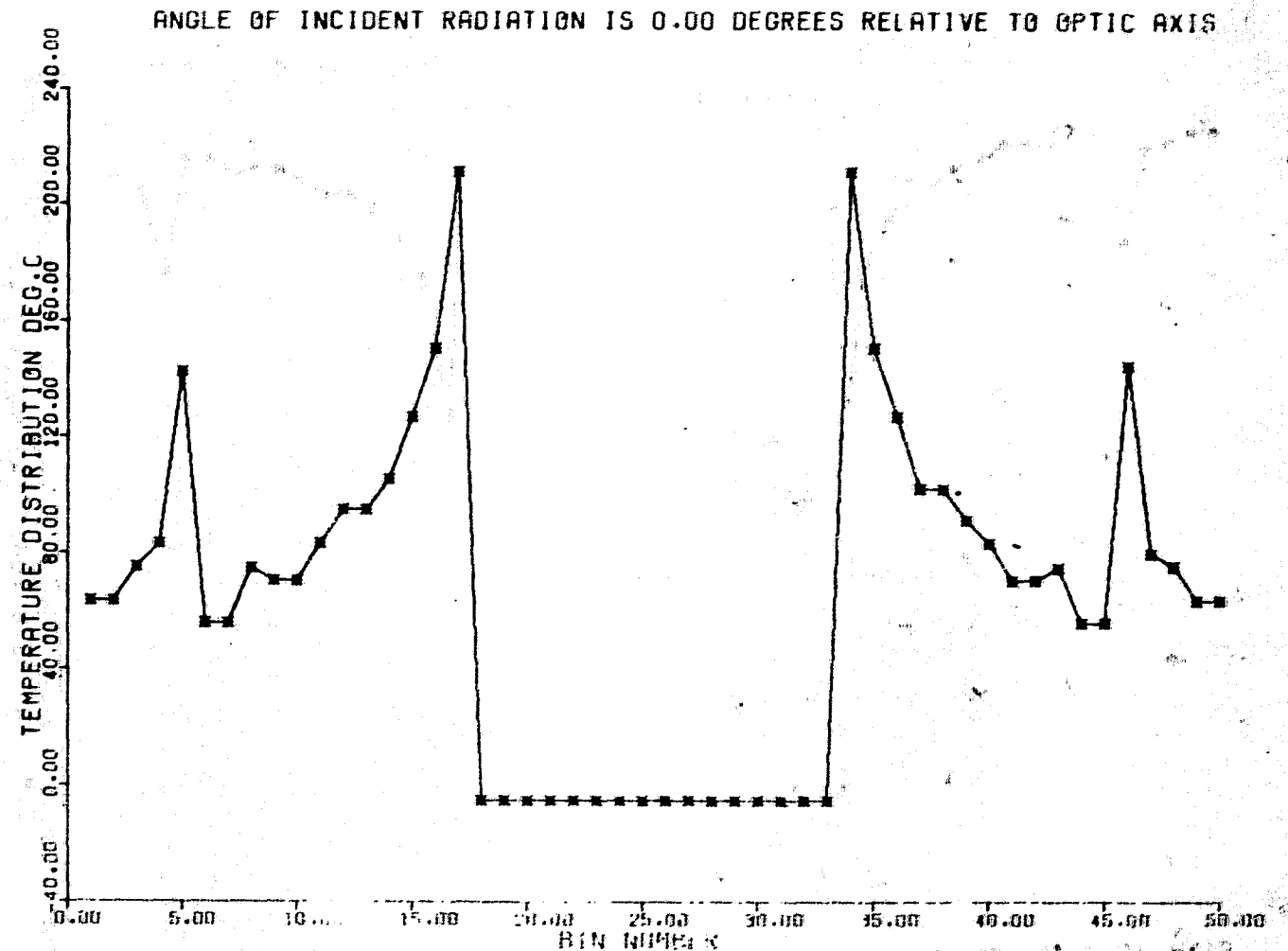

Figure B-14. Temperature vs Bin No. for Theta = 8.2 deg Configuration

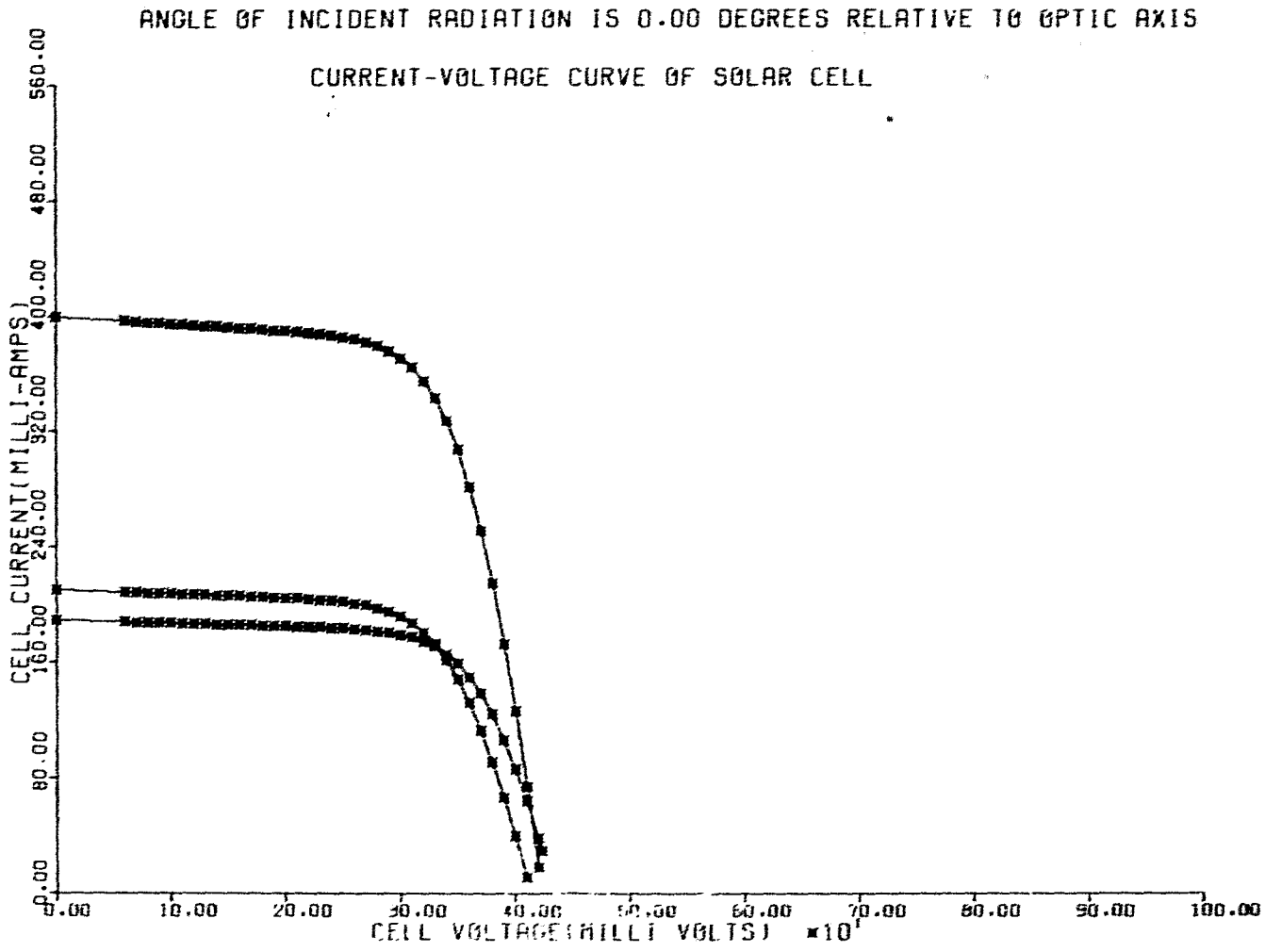

Figure B-15. Array I-V Curve for Theta = 8.2 deg

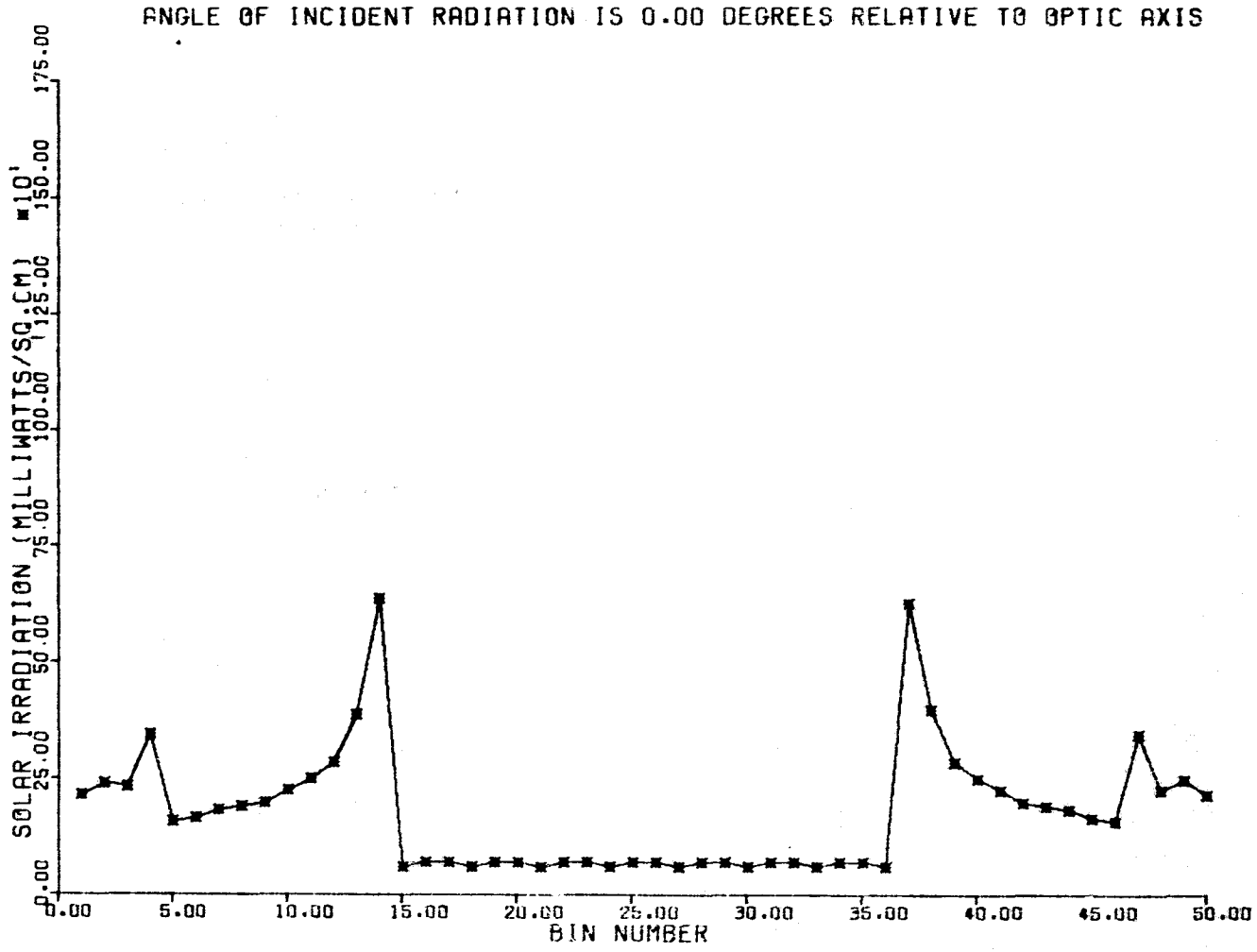

Figure B-16. Intensity vs Bin No. for Theta = 10.3 deg Configuration

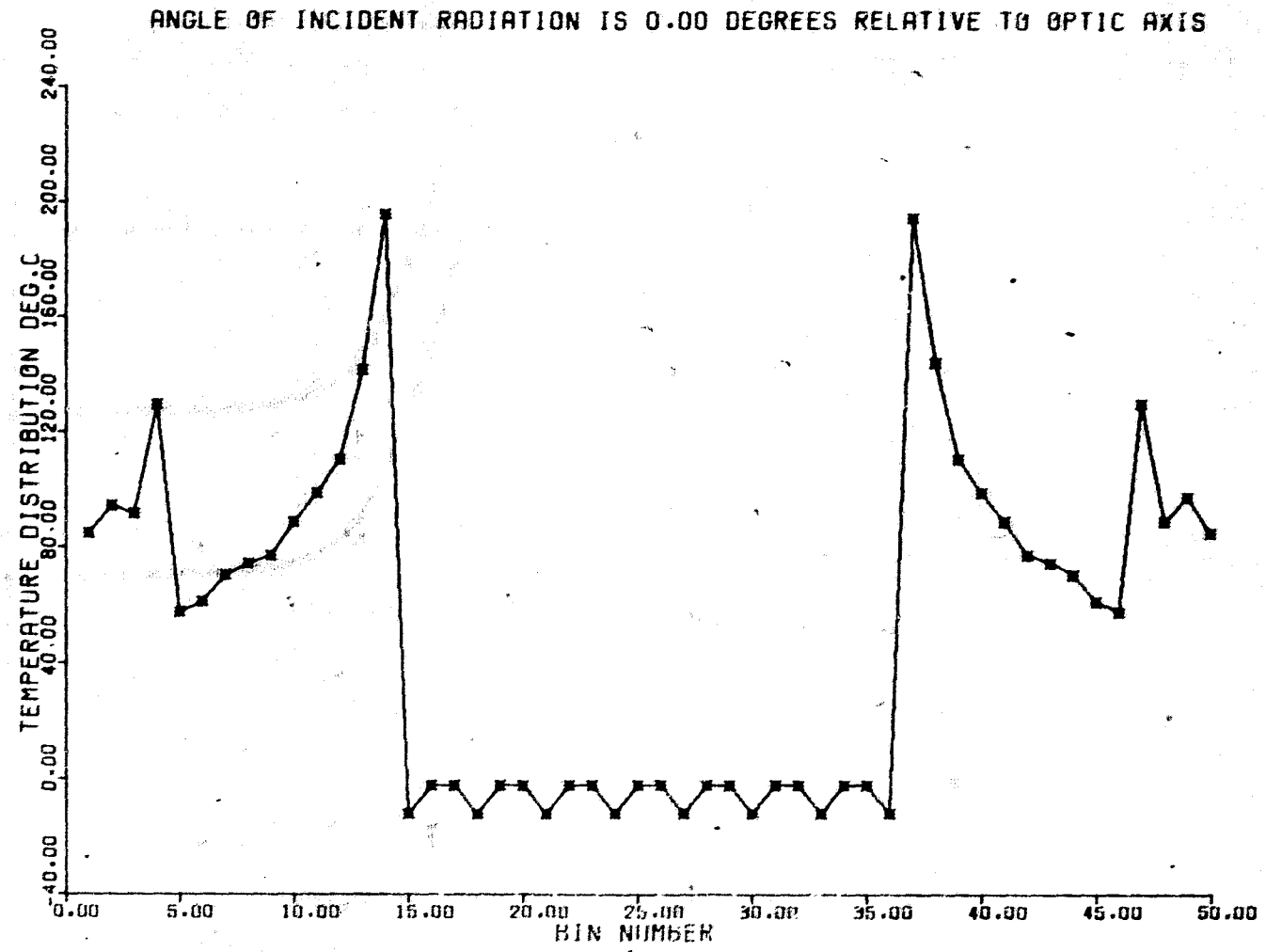

Figure B-17. Temperature vs Bin No. for Theta = 10.3 deg Configuration

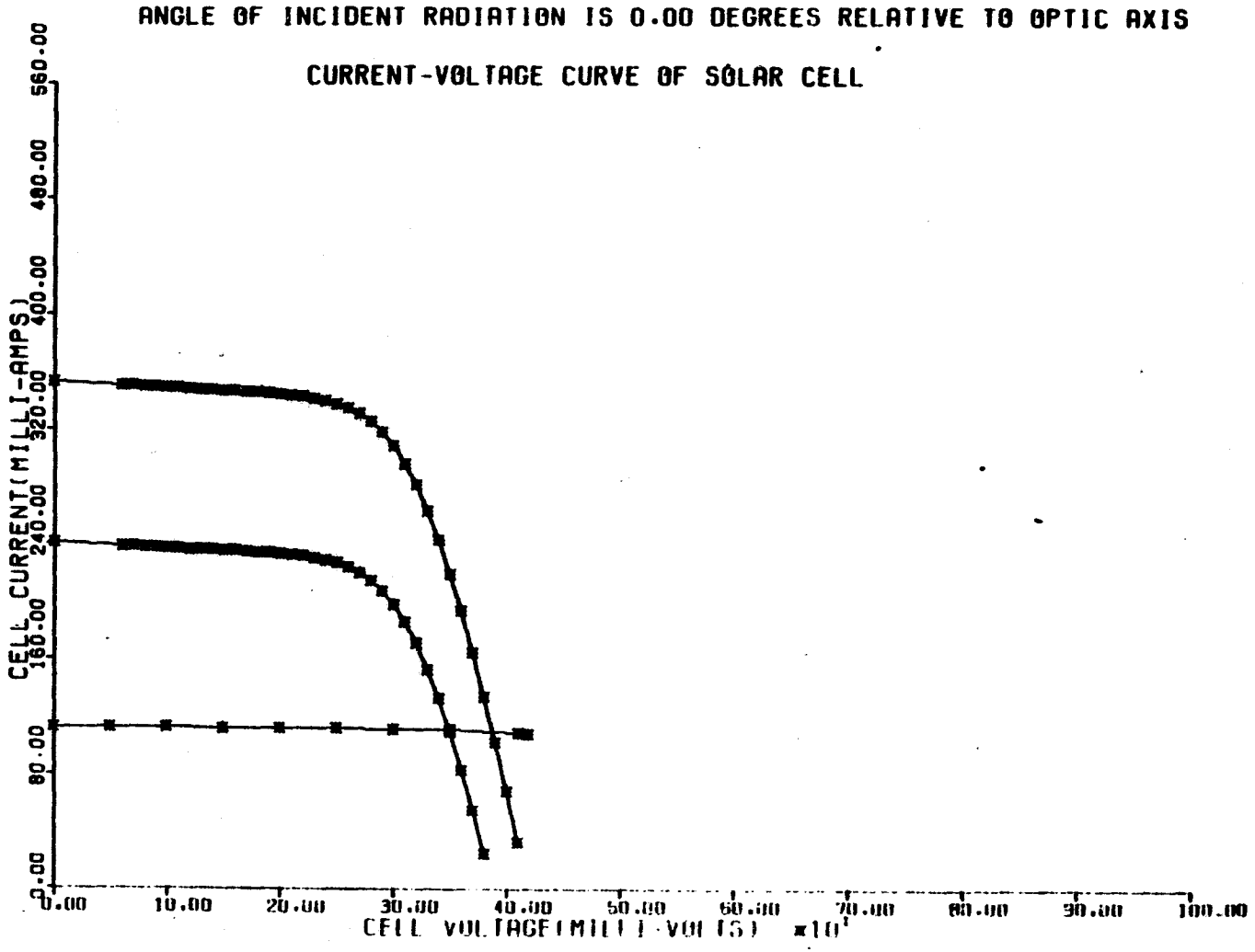

Figure B-18. Array I-V Curve for Theta = 10.3 deg

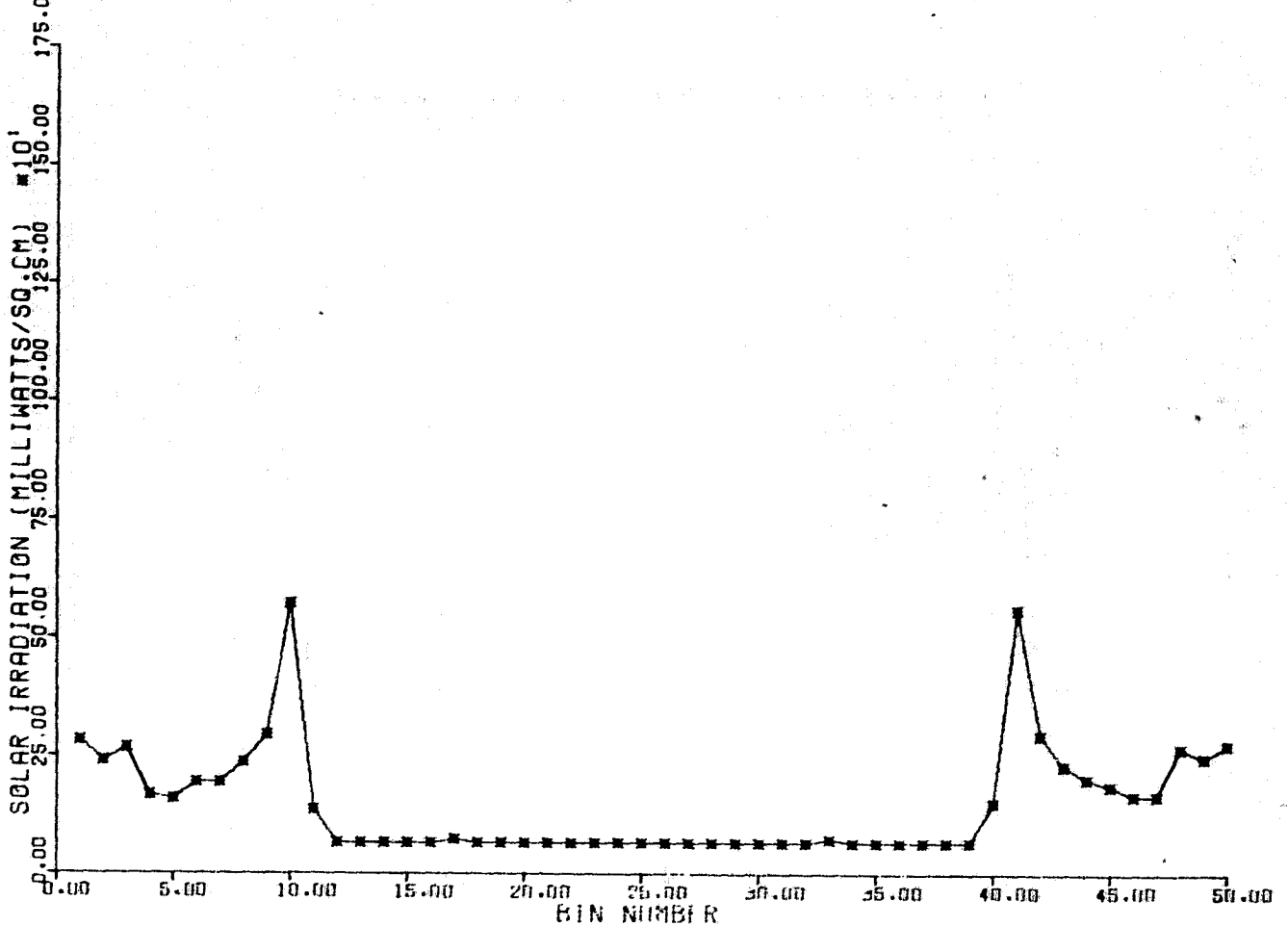

Figure B-19. Intensity vs Bin No. for Theta = 13.5 deg Configuration

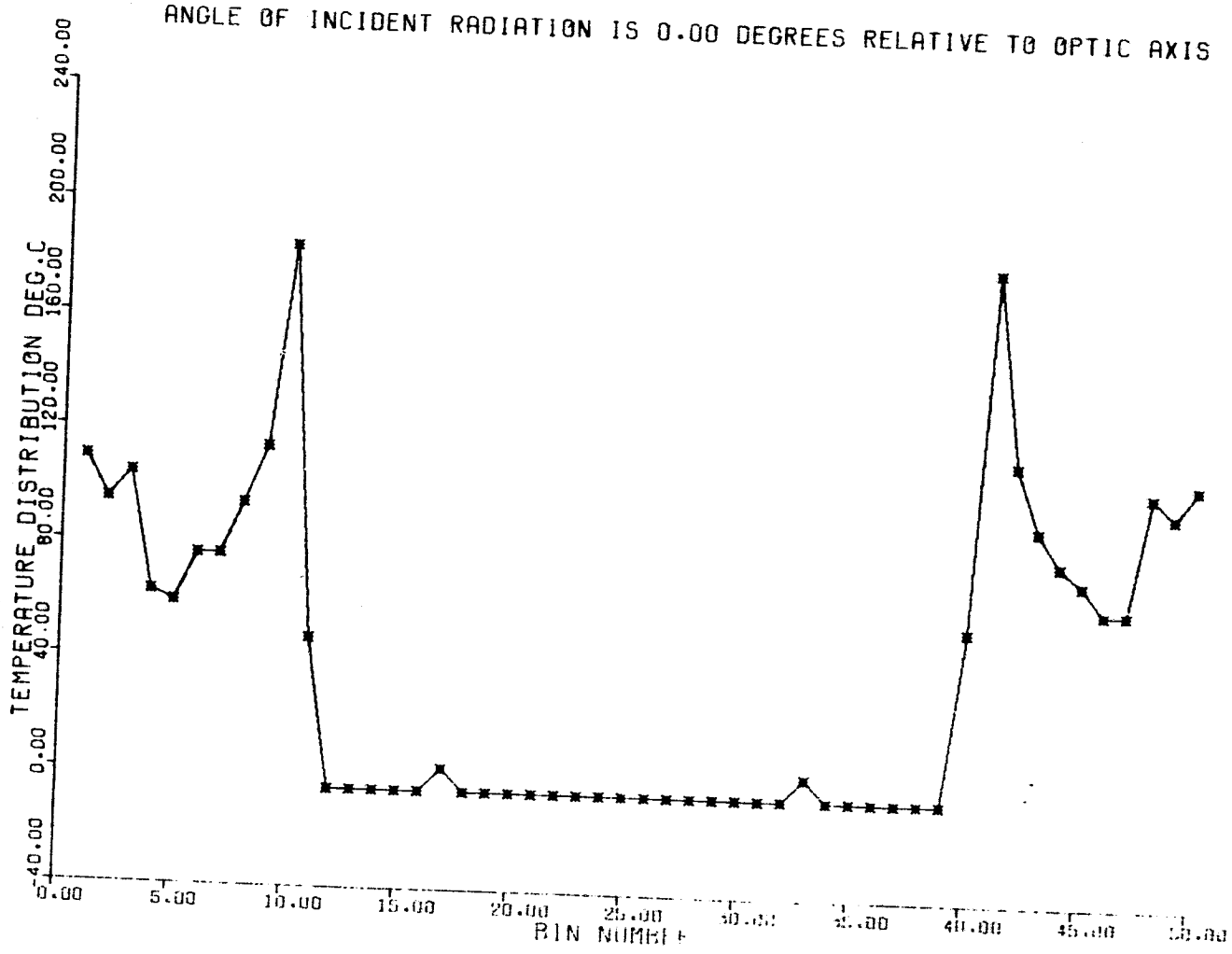

Figure B-20. Temperature vs Bin No. for Theta = 13.5 deg Configuration

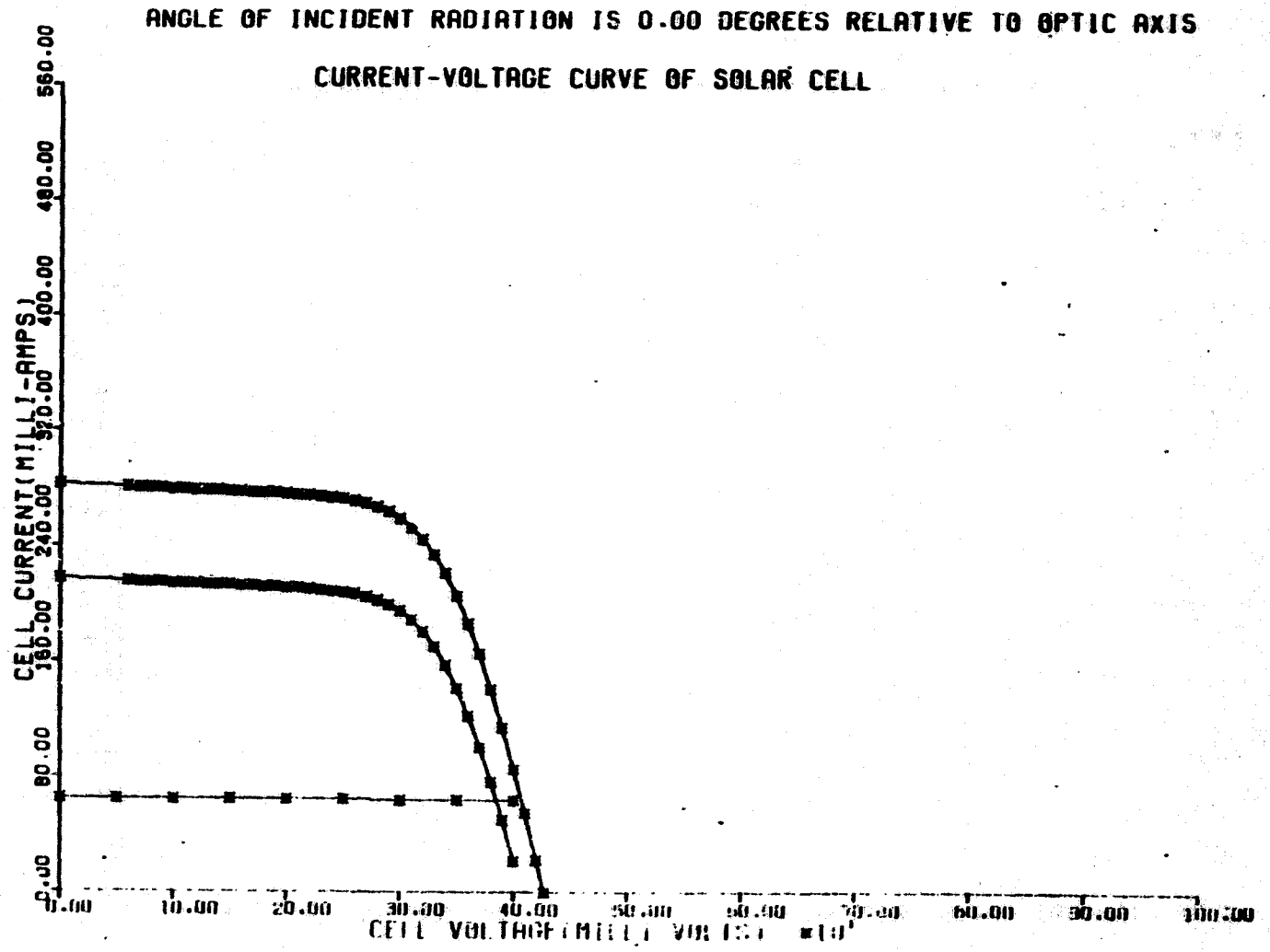

Figure B-21. Array I-V Curve for Theta = 13.5 deg

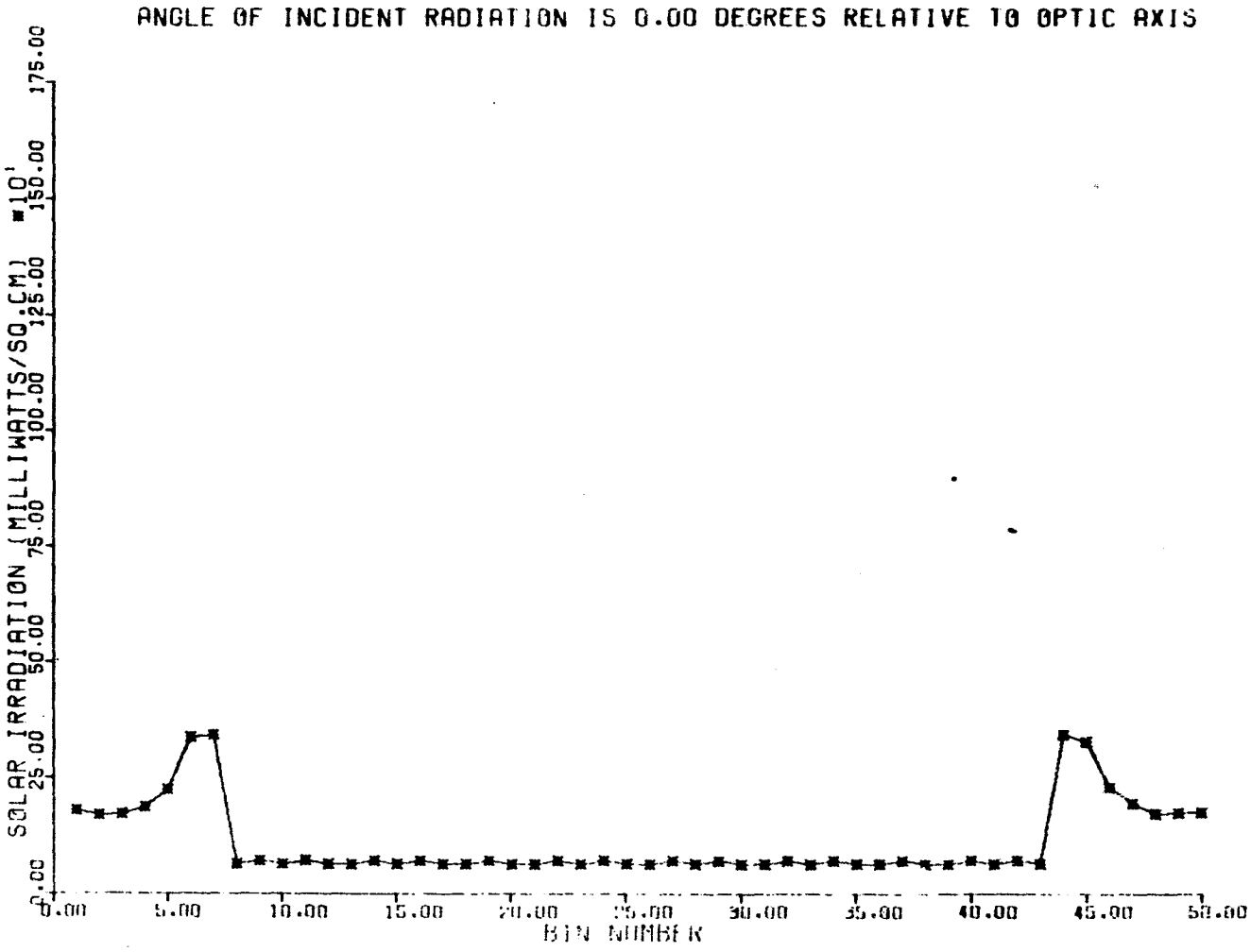

Figure B-22. Intensity vs Bin No. for Theta = 17.9 deg Configuration

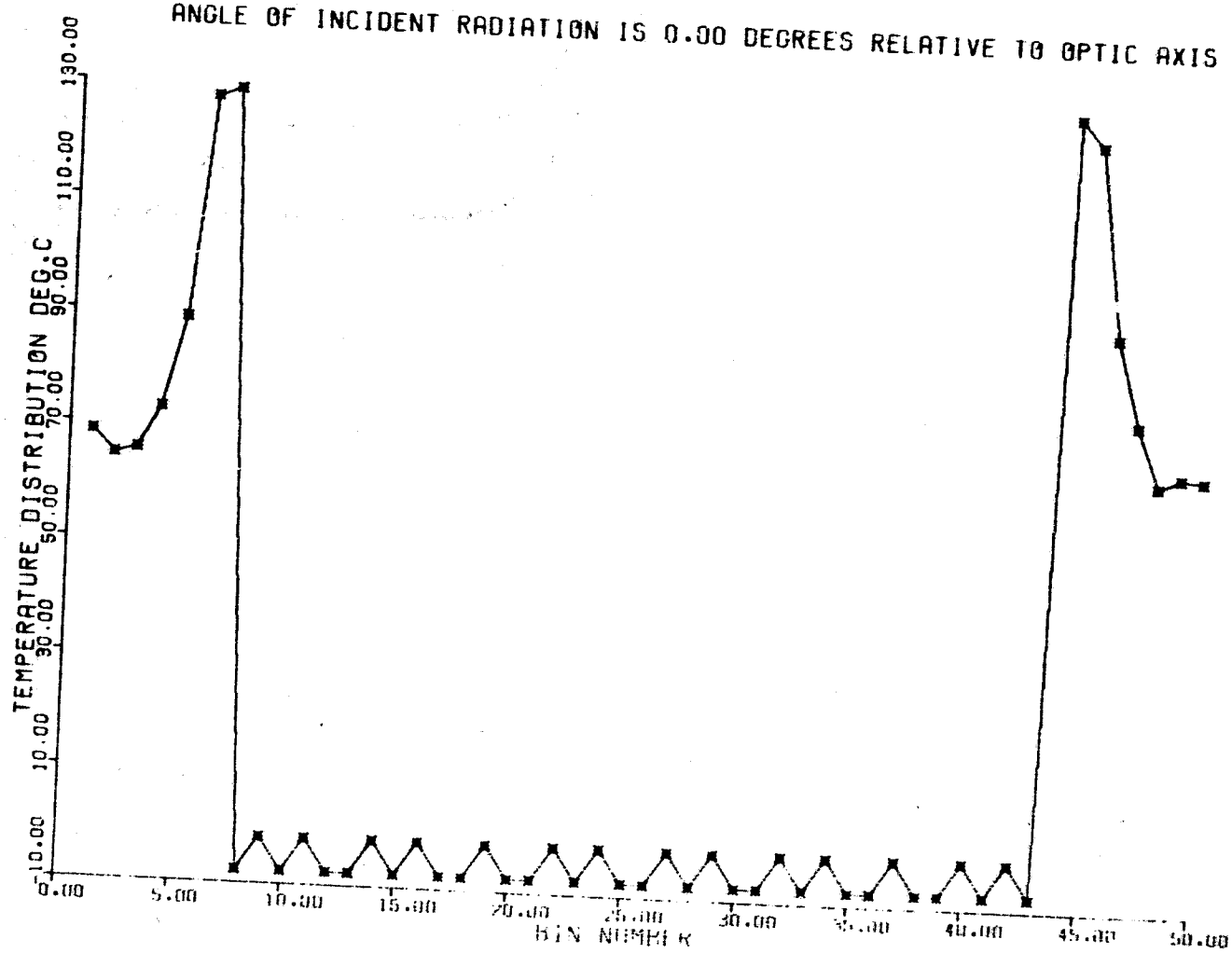

Figure B-23. Temperature vs Bin No. for Theta = 17.9 deg Configuration

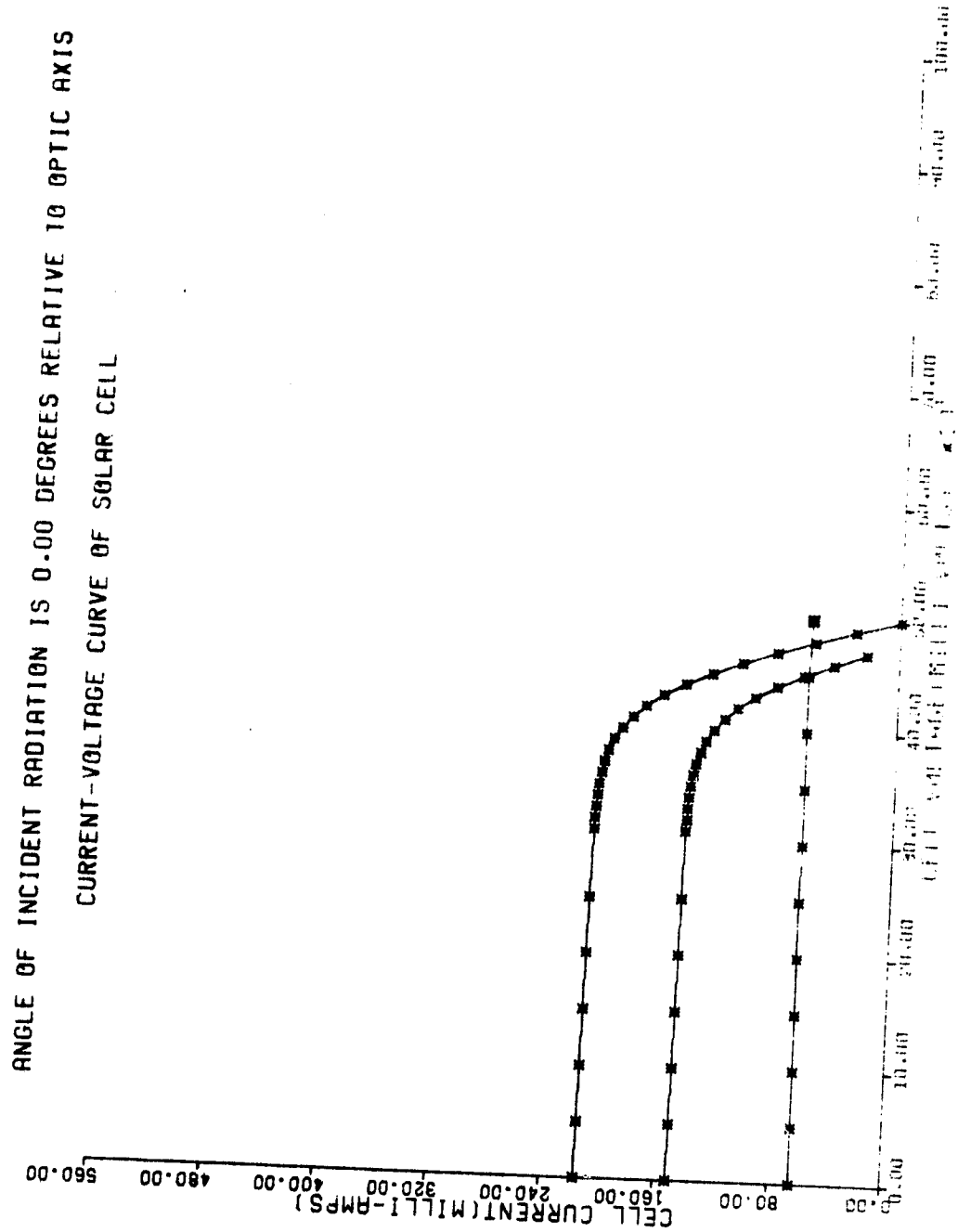

Figure B-24. Array I-V Curve for Theta = 17.9 deg

NASA—JPL—Coml., L.A., Calif.